Used Fuel Disposition Campaign

Phase I Ring Compression Testing of High-Burnup Cladding

Fuel Cycle Research & Development

Prepared for
U.S. Department of Energy
Used Fuel Disposition Campaign

M.C. Billone, T.A. Burtseva,
J.P. Dobrzynski, D.P. McGann,
K. Byrne, Z. Han, and Y.Y. Liu

Argonne National Laboratory
December 31, 2011
FCRD-USED-2012-000039

Reviewed by:

Digitally signed by Hanchung Tsai
DN: cn=Hanchung Tsai, o=ANL, ou=DIS, email=htsai@anl.gov, c=US
Date: 2012.01.10 09:19:49 -06'00'

Hanchung Tsai (Argonne National Laboratory)
Technical Reviewer

Submitted by:

Yung Y. Liu (Argonne National Laboratory)
Work Package Manager for Engineering Materials Experimental

Page intentionally blank

SUMMARY

The purpose of ring compression testing is to generate data to support the development of the technical basis for extended storage and transportation of high-burnup fuel. Argonne National Laboratory developed the methodology of using ring compression tests (RCTs) for radial-hydride-treated (RHT) cladding to generate data for the Nuclear Regulatory Commission (NRC) on the behavior of high-burnup Zircaloy-4 (Zry-4) and ZIRLO™ cladding. The RHT/RCT methodology is an established test protocol accepted by NRC for generating data to support the technical basis for licensing storage and transportation casks with high-burnup fuel. In July 2011, Phase I testing for DOE on high-burnup M5® cladding was initiated under the ANL FY11 Work Package Transportation; Phase I testing for DOE on high-burnup M5® cladding continued into fiscal year 2012 under the ANL FY12 Work Package Engineering Materials Experimental. This report highlights the results of completed Phase I testing of high-burnup M5® cladding and the revised three-year test plan, which is included in the Appendix.

Relative to lower-burnup fuel, high-burnup (≥45 GWd/MTU) used fuel rods are characterized by increased: decay heat following reactor discharge, internal gas pressure, cladding corrosion-layer thickness, and cladding hydrogen content. Under pool-storage conditions following reactor discharge, hydrogen in fuel cladding will be in the form of hydrides precipitated in the circumferential direction. Circumferential hydrides, in combination with irradiation-induced hardening, decrease cladding ductility in response to axial and hoop loads, but high-burnup cladding still retains a low level of ductility. At elevated temperatures (≤400°C) during drying-transfer operations and the early stage of dry-cask storage, the internal gas pressure and cladding hoop stress increase, as some of the hydrogen goes into solution (e.g., about 200 wppm at 400°C). During cooling under tensile hoop stress, some of the dissolved hydrogen will re-precipitate in the radial direction across the cladding wall if the hoop stress is high enough. After cooling to about 200°C, essentially all the dissolved hydrogen will have re-precipitated. Further cooling during storage may result in radial-hydride-induced embrittlement at <200°C. The temperature at which embrittlement occurs is termed the ductile-to-brittle transition temperature (DBTT). Hoop stress loading may be high enough to cause brittle cladding failure and fuel dispersal during post-storage retrieval, transport, and post-transport retrieval of used fuel rods.

Conditions that may lead to cladding radial-hydride formation and embrittlement are described in Section 5.2.3.5 of *Gap Analysis to Support Extended Storage of Used Fuel* (Hanson et al. 2011). The importance of conducting R&D in this area is ranked as high (see Table S-1 in report). On April 28, 2011, Argonne issued a three-year test plan ("Provisional Test Plan for High-Burnup Fuel Cladding and Modeling") to address this data gap. The test plan builds on the in-depth knowledge and experience gained in performing ring compression testing for NRC with high-burnup cladding. Phase I ring compression testing for DOE focused on high-burnup M5® following simulated drying/transfer-storage within cladding temperature limits established by NRC in Interim Staff Guidance – 11 (Revision 3). Subsequent ring compression testing will focus on high-burnup cladding (Zry-4, ZIRLO™, M5®, and Zry-2) at and below current ISG-11 (Rev. 3) limits for temperature and temperature cycling. The goal of the ring compression testing is to identify process conditions that would minimize radial-hydride formation and the corresponding DBTT of high-burnup fuel cladding and to generate data and models to support the development of the technical basis for extended storage and transportation of high-burnup fuel, including fuel retrievability.

Page intentionally blank

CONTENTS

FIGURES

FIGURES (Cont.)

FIGURES (Cont.)

Page intentionally blank

1. INTRODUCTION

Fuel rods with burnup levels ≥45 GWd/MTU are classified as high burnup. Relative to lower-burnup fuel rods, high-burnup fuel rods are characterized by increased: decay heat following reactor discharge, internal gas pressure, cladding corrosion (outer-surface oxide) layer thickness, and cladding hydrogen content. Under pool-storage conditions following reactor discharge, hydrogen in used fuel cladding will be in the form of precipitated hydrides, which are primarily oriented in the circumferential direction. Circumferential hydrides, along with hardening of the base metal due to irradiation, will decrease cladding ductility to a low level in response to axial and hoop loads. At elevated temperatures (≤400°C) during drying and transfer operations and the early stage of dry-cask storage, the internal gas pressure and cladding hoop stress increase, as some of the hydrogen goes into solution (e.g., about 200 wppm at 400°C). During cooling under tensile hoop stress, some of the dissolved hydrogen will precipitate in the radial direction across the cladding wall if the hoop stress is high enough. After cooling to about 200°C, essentially all of the dissolved hydrogen will have re-precipitated as hydrides. Further cooling during storage may result in radial-hydride-induced embrittlement at <200°C. The temperature at which embrittlement occurs is termed the ductile-to-brittle transition temperature (DBTT). During storage, hoop stresses are too low to fail the cladding. However, hoop-stress loading may be high enough to cause brittle cladding failure during post-storage retrieval, cask transportation accidents (i.e., cask drops >0.3 m), and possibly post-transportation retrieval and repackaging.

Issues associated with the decrease in cladding ductility following irradiation to high burnup and with possible embrittlement following drying/transfer operations and extended long-term storage in dry casks are addressed in the draft report *Gap Analysis to Support Extended Storage of Used Nuclear Fuel* (Hanson et al. 2011). These issues and other related matters are summarized in the following subsections.

1.1 Characteristics of High-Burnup Cladding

The corrosion-layer thickness and associated hydrogen pickup for cladding from fuel rods irradiated to high burnup depend on the cladding alloy composition, coolant temperature, fuel-rod linear power and heat flux history, and in-reactor residency time. For boiling water reactors (BWRs), the coolant temperature is relatively low (≈290°C) and constant along most of the fuel-rod length. BWR Zircaloy-2 (Zry-2) cladding has a corrosion-layer thickness of about 10 to 60 μm and associated hydrogen content of 100 to 300 wppm at the licensed discharge burnup of 62 GWd/MTU (Tsai and Billone 2003; Nakatsuka et al. 2004). Most modern Zry-2 cladding is recrystallized-annealed (RXA) and has an inner liner of zirconium (about 10% of the wall thickness). The resulting hydrogen concentration for high-burnup BWR cladding is very high in the inner-surface Zr liner, low within the inner half of the cladding wall, and intermediate within the outer half of the cladding wall.

Pressurized-water-reactor (PWR) cladding is exposed to higher coolant temperature (about 300°C inlet and 330°C outlet). In general, this leads to thicker corrosion layer and higher hydrogen pickup, as well as significant axial variation along the lengths of the fuel rods. High-burnup PWR cladding is characterized by a coolant-side corrosion layer (10 to 100 μm thick), a dense hydride rim (for >150 wppm hydrogen pickup), a radiation-hardened zirconium-alloy matrix with a low concentration of hydrides (<140 wppm), and a thin fuel-side oxide layer, which contains fission products and actinides. Corrosion-layer thickness and hydrogen pickup are highly dependent on alloy type, coolant temperature, heat flux, and residency

time in the reactor. Zr-1Nb alloys such as M5® have low corrosion-layer thickness (≤20 μm) and hydrogen pickup (≤100 wppm), while Zr-1.3Sn alloys such as low-tin Zircaloy-4 (Zry-4) have high corrosion-layer thickness (≤100 μm) and hydrogen pickup (600-1000 wppm) at the same burnup and under the same operating conditions. Zr-1Nb-1Sn alloys such as ZIRLO™ have lower corrosion-layer thickness as compared to Zry-4 under the same operating conditions, but the alloy may have a higher hydrogen pickup fraction. For aggressive operating conditions, ZIRLO™ has peak corrosion-layer thickness values of 40 to 60 μm and peak hydrogen pickup of 400 to 600 wppm.

Cladding hydrides at room temperature are basically in the form of platelets oriented in the circumferential direction. Examples of hydride distribution and hydrogen content for high-burnup PWR cladding alloys (Zry-4, ZIRLO™, and M5®) are shown in Figures 1-4 (Billone et al. 2008; Yan et al. 2009). From Figure 1, it can be seen that the corrosion layer and hydrogen content for Zry-4 at 64 GWd/MTU increase significantly with axial location due to the increase in coolant temperature. Although most of the hydrogen is contained in the outer third of the Zry-4 wall, the hydride rim is not as localized as it is for other higher-burnup cladding. This distribution may be due to the lower temperature gradient across the cladding wall for the burnup increase from 45 to 64 GWd/MTU. The fuel enrichment was only 2.9% U-235 and the rod was irradiated for seven reactor cycles (about 2300 effective full-power days). Figure 2 shows the hydride morphology and distribution for ZIRLO™ cladding from a fuel rod irradiated to 70 GWd/MTU and at an axial location where the hydrogen pickup was 660 wppm for a 43-μm-thick corrosion layer. The hydride rim is denser and more concentrated at the outer surface for this 4% U-235 enriched fuel, which was irradiated for four reactor cycles. At a location about 0.7 m lower on the rod (Figure 3), the hydrogen content (320 wppm) and corrosion-layer thickness (26 μm) were considerably smaller than at the higher axial location. However, the hydride rim was well developed at both of these axial locations. The increase in hydrogen content manifested itself as an increase in hydride rim thickness with little change (estimated from metallographic images) in hydrogen content in the bulk of the cladding below the rim. Both high-burnup ZIRLO™ and Zry-4 cladding exhibit the same trends with regard to increase in hydrogen content with increase in axial elevation. Figure 4 shows the low corrosion-layer thickness (12 μm) and hydrogen pickup (100 wppm) for M5® from a fuel rod irradiated to 63 GWd/MTU. In terms of texture, M5® cladding is RXA, while Zry-4 and ZIRLO™ cladding alloys are cold-worked/stress-relieved-annealed (CWSRA) materials. The high-burnup cladding characterizations described in this section apply to fuel discharged from the reactor and stored in spent-fuel pools prior to drying/transfer operations and dry-cask storage.

It is interesting to note that cladding with less than about 350 wppm hydrogen has a relatively small circumferential variation (about 10%) in hydrogen content. However, cladding with >450 wppm hydrogen has a significant circumferential variation. On the basis of measurements for four quarter-arc segments, the hydrogen contents for Zry-4 in Figure 1 were 550±100 wppm near the fuel mid-plane and 740±110 wppm at about 0.7 m above the fuel mid-plane. Using the same technique for ZIRLO™ (see Figures 2 and 3), the hydrogen contents were measured to be 660±150 wppm and 320±30 at about 1.1 m and 0.4 m, respectively, above the fuel mid-plane.

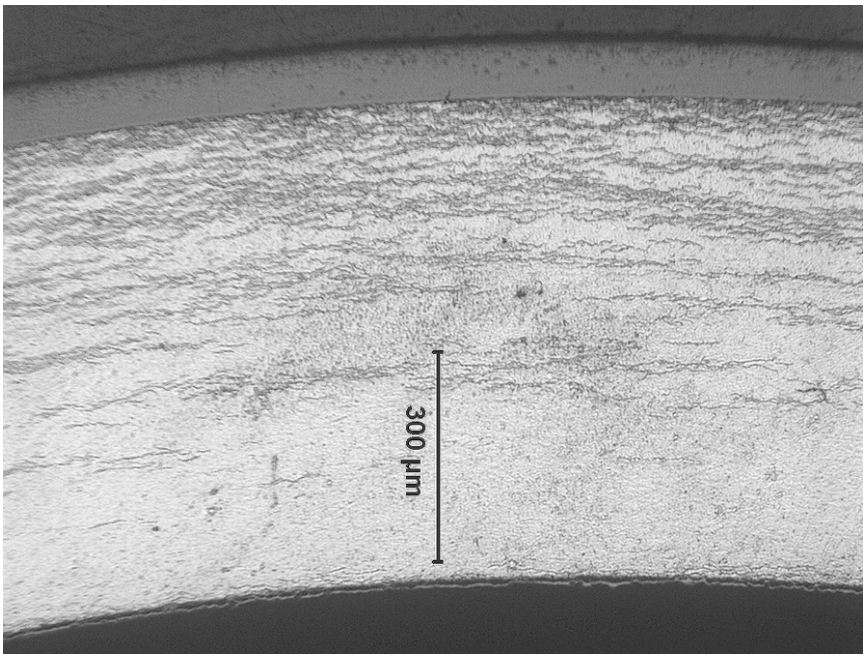

(a) Fuel mid-plane

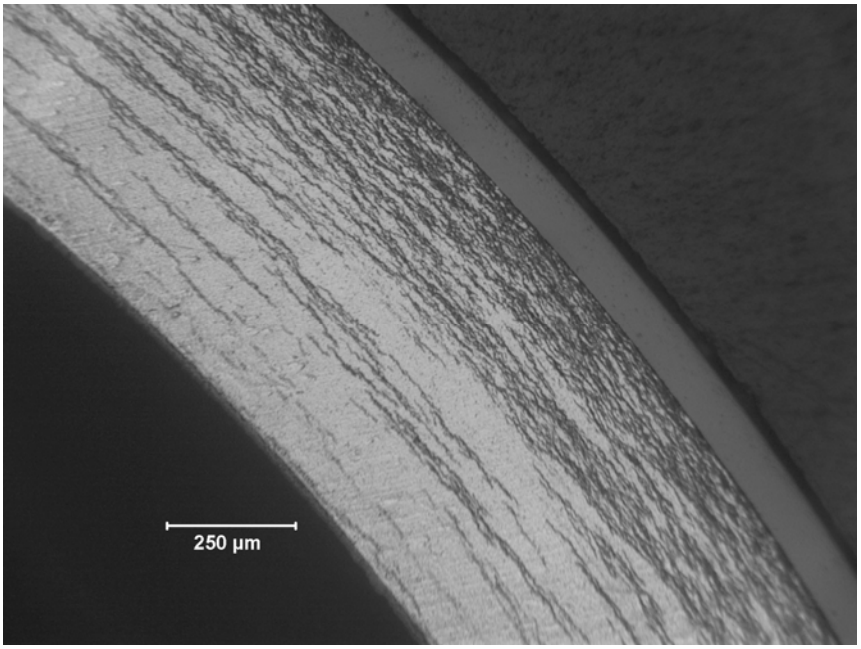

(b) 0.65 m above fuel mid-plane

Figure 1. Hydride distribution and morphology in Zry-4 cladding from a high-burnup fuel rod irradiated to 64 GWd/MTU in one of the H. B. Robinson reactors: (a) fuel mid-plane (550 wppm H); (b) 0.65 m above mid-plane (740 wppm H). The corresponding corrosion-layer thicknesses are 71 and 95 µm (Billone et al. 2008).

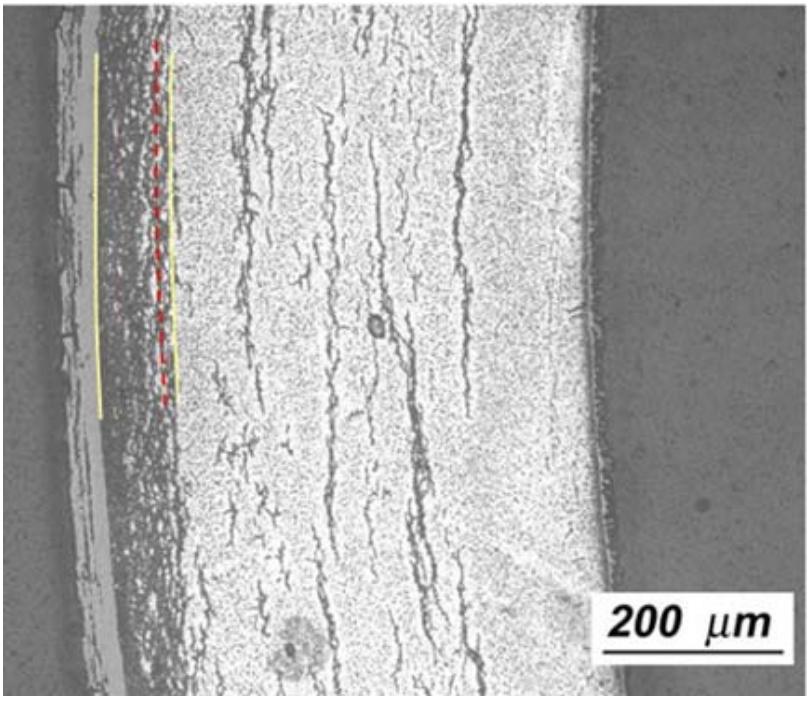

(a) Thick hydride rim at about 1.1 m above fuel mid-plane

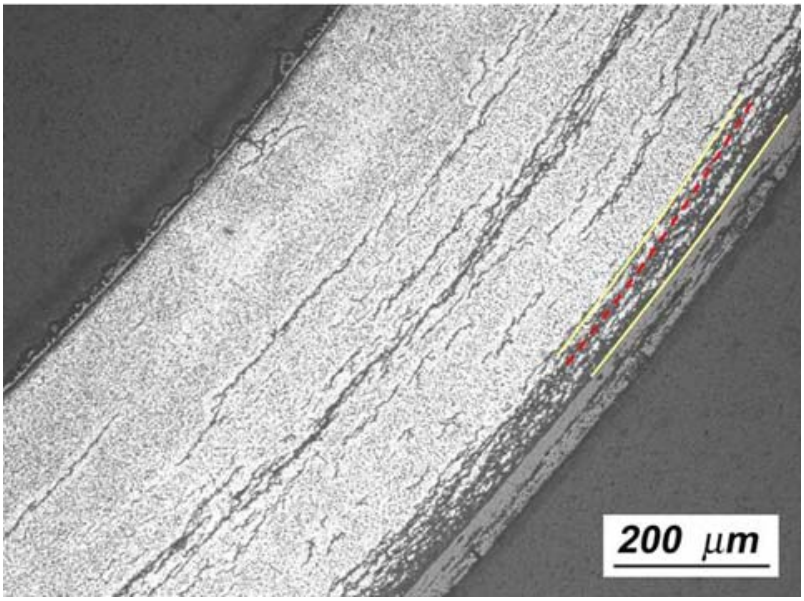

(b) Thin hydride rim at the same axial location (1.1 m above fuel mid-plane)

Figure 2. Hydride distribution and morphology in ZIRLO™ cladding from a high-burnup fuel rod irradiated in the North Anna reactors to 70 GWd/MTU: (a) circumferential region with thickest (≈70 μm equivalent) hydride rim; (b) circumferential location with thinnest (≈40 μm equivalent) hydride rim. The red dashed lines in the images were used to estimate equivalent (i.e., dense) thickness. The average hydrogen content at this location was 660 wppm with local circumferential values from 500 to 840 wppm. The corresponding corrosion layer was 43 μm thick (Billone et al. 2008).

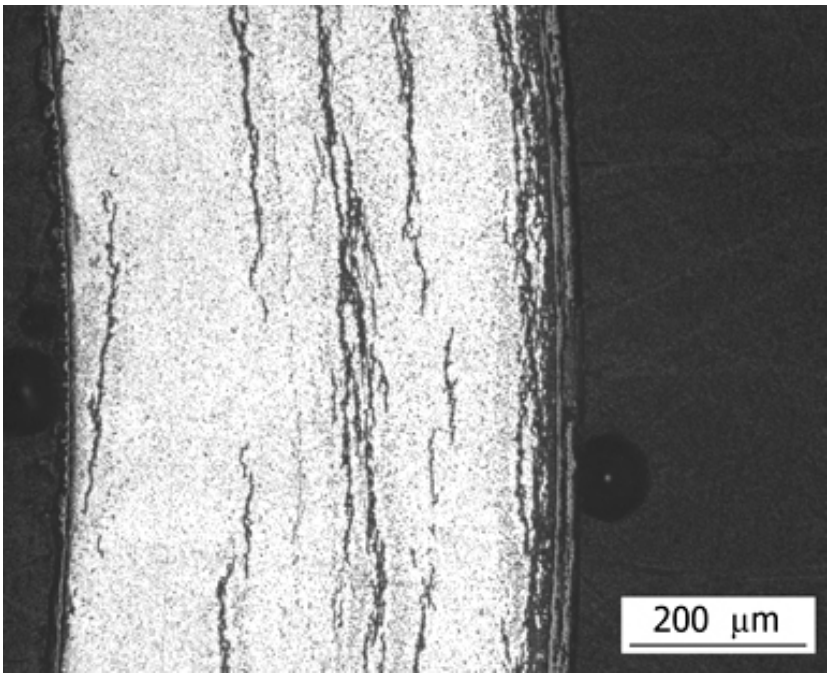

(a) Circumferential hydrides

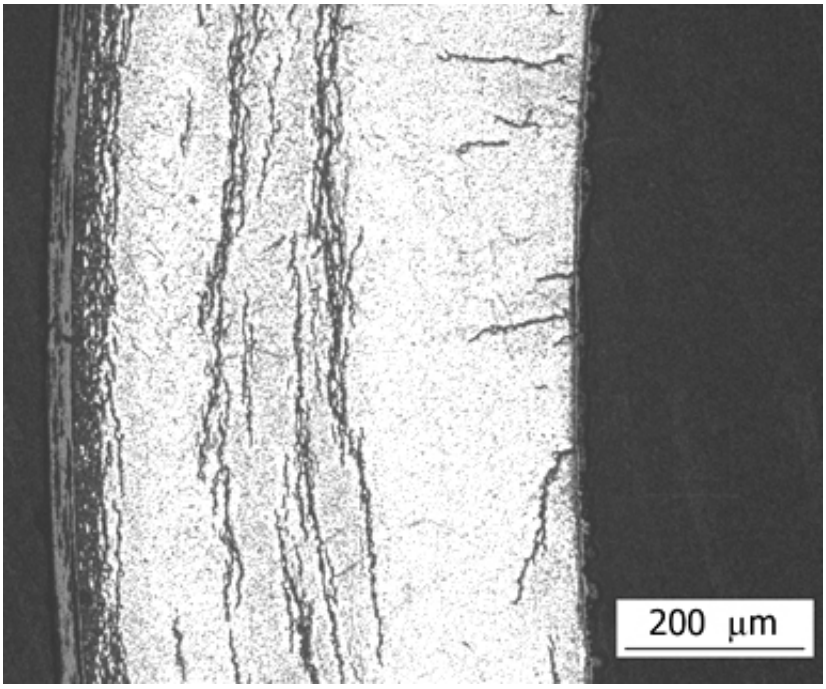

(b) Circumferential and radial hydrides

Figure 3. Hydride distribution and morphology at 0.44 m above the fuel mid-plane for ZIRLO™ cladding from a high-burnup fuel rod irradiated in the North Anna reactors to 70 GWd/MTU: (a) circumferential location with typical (7 out of 8 images) circumferential hydride orientation; (b) circumferential location with local region of circumferential and radial hydrides. The average hydrogen content at this location was 320 wppm and the corresponding corrosion layer was 26 µm thick (Yan et al. 2009).

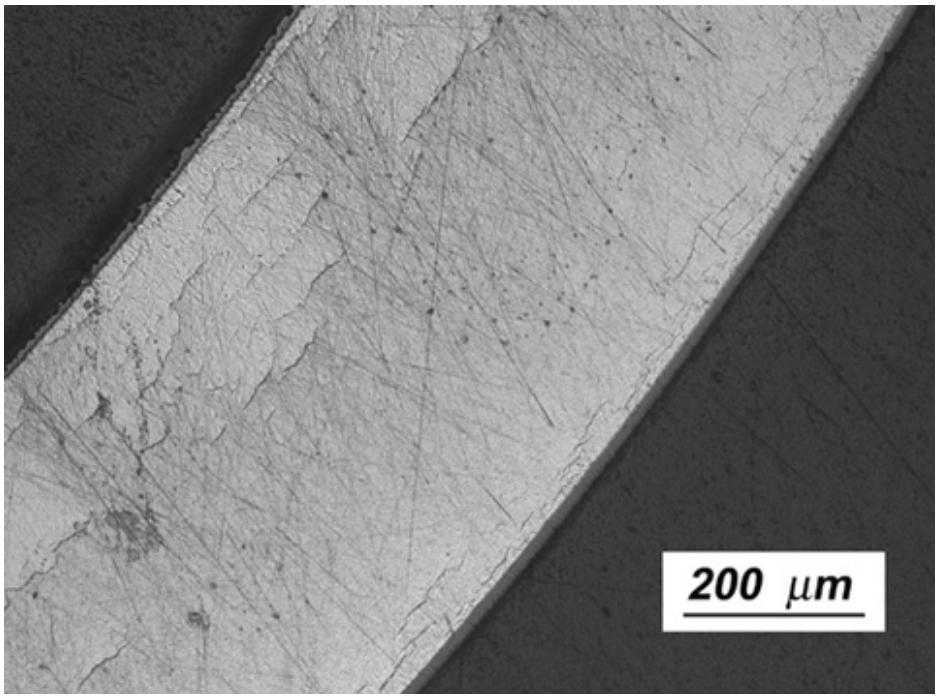

(a) Circumferential hydrides

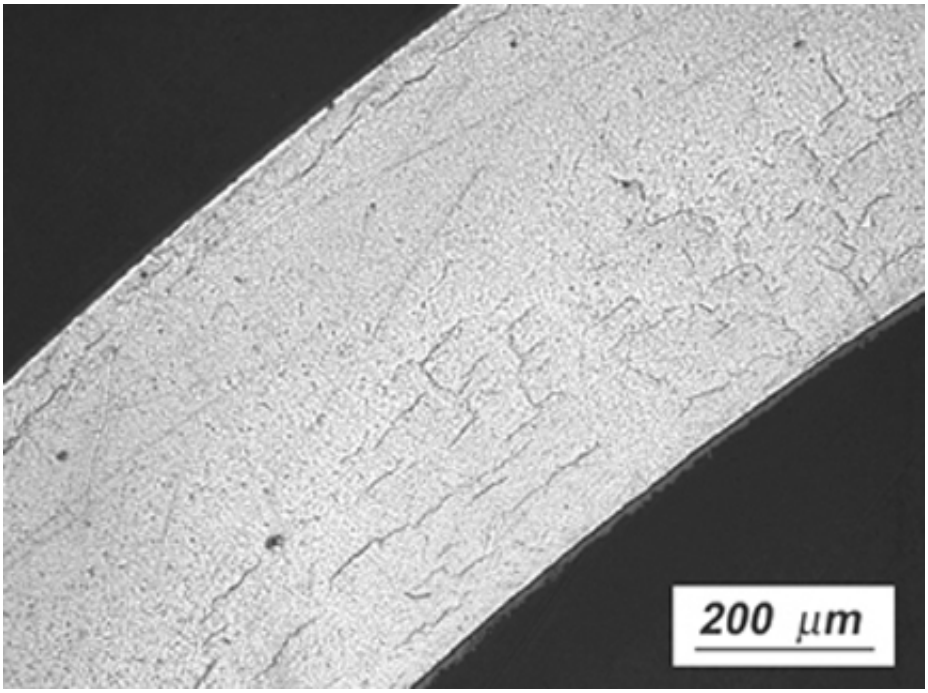

(b) Circumferential and radial hydrides

Figure 4. Hydride distribution and morphology at 3.0 m above rod bottom for M5® cladding from a high-burnup fuel rod irradiated in one of the Ringhals reactors to 63 GWd/MTU: (a) local region with typical (7 out of 8 images) circumferential hydrides; (b) local region with circumferential and radial hydrides. The average hydrogen content was 100 wppm and the corresponding corrosion layer was 12 μm thick (Billone et al. 2008).

1.2 High-Burnup Fuel-Rod Gas Pressures and Hoop Stresses

At full power, internal gas pressures are limited by fuel-vendor design specifications to prevent cladding "liftoff" from the fuel due to internal gas pressures higher than the coolant pressure. The coolant pressures for BWRs and PWRs are 7.17 MPa (1040 psia) and 15.5 MPa (2250 psia), respectively. Early design criteria limited most of the fuel rods to pressures ≤ the coolant pressure and a limited number of rods to ≤ 1.3 times the coolant pressure. The 1.3 factor would give 9.32 MPa (1350 psia) and 20.2 MPa (2825 psia) for BWRs and PWRs, respectively. However, it was later determined that these limits were too conservative, especially for BWR fuel rods, and the rod pressure limits were increased to 13.8 MPa (2000 psia) and 21.7 MPa (3150 MPa) for BWRs and PWRs, respectively (Beyer and Montgomery 2011). In meeting these limits, fuel vendors very conservatively estimate the upper-bound fission gas release. Although the dataset for high-burnup fuel-rod internal pressure is limited, the results suggest that actual pressures in high-burnup fuel rods are considerably less than those based on the upper-bound values.

Internal gas pressure is an important parameter in determining cladding hoop stress during elevated-temperature drying/transfer and the early stage of dry-cask storage. In developing test matrices for cladding alloys, it is desirable to avoid testing at pressures above the vendor- and utility-imposed limits. These limits apply to full-power operation during which most of the gas is in the plenum region at temperatures of 290°C and 330°C for high-burnup BWR and PWR fuel rods, respectively. During drying/transfer operations and storage, the cladding plenum region will be at a lower temperature than the peak cladding temperature, which is limited to 400°C. Given the conservatism in the 21.7-MPa pressure limit for PWR fuel rods at about 330°C, it would be too conservative to extrapolate this pressure to 400°C. However, for BWR fuel rods, the 13.8 MPa is extrapolated to 330°C to give 15.4 MPa under peak cladding drying/transfer-storage conditions. Converting these PWR and BWR pressures to hoop stresses gives 160 MPa and 120 MPa, respectively, for peak cladding stresses during drying operations and storage.

For testing purposes, it is reasonable to test within the range from half the limiting pressure to the full limiting pressure. This would give 80 to 160 MPa for PWR cladding and 60 to 120 MPa for BWR cladding.

1.3 Mechanical Properties of As-Irradiated Cladding

Increased burnup leads to increased fast-neutron fluence and hydrogen content. Exposure to fast neutrons results in classical irradiation hardening and decrease in ductility, as well as hardening increase and ductility decrease due to changes in second phase precipitates. The ductility also continues to decrease with increasing hydrogen-content levels. References for axial and hoop mechanical properties of high-burnup cladding are given in subsection 5.2.3.5 of the draft report by Hanson et al. 2011. However, it is important to emphasize that these mechanical properties apply to irradiated cladding discharged from the reactor and pool-stored prior to defueling and testing cladding samples. As discussed in Section 1.1 of this report, the hydride orientation in such cladding is primarily circumferential. Such an orientation is much less detrimental to cladding ductility in the hoop direction than hydrides oriented in the radial direction.

Most cask vendors use the mechanical properties developed by PNNL (Geelhood et al. 2008 or earlier versions of the PNNL compilations) for Zircaloy cladding. The data used to compile stress-strain properties were primarily for irradiated CWSRA Zry-4. Limited data for irradiated RXA Zry-2 were also used. In the opening paragraph of the introduction, the authors state in bold letters: "**The models described here apply only to cladding with circumferential hydrides and do not apply to cladding with radial hydrides….**"

The primary reason for the PNNL disclaimer is that radial hydrides can cause brittle failure of cladding in the elastic deformation regime in response to hoop loading. Engineering stress-strain parameters such as yield strength, ultimate tensile strength, uniform elongation, and total elongation would not be relevant as these properties are derived for cladding that exhibits plastic deformation prior to failure. Thus, it is very important to determine the drying/transfer-storage conditions for which radial-hydride-induced embrittlement occurs during and after cooling.

1.4 Review of Previous Studies of Radial Hydride Embrittlement

The open literature contains many articles giving research results for non-irradiated, pre-hydrided cladding alloys. During the pre-hydriding process, temperature cycling is used to distribute hydrogen uniformly across the cladding wall. However, high-burnup fuel with greater than about 200 wppm hydrogen has a very different distribution of hydrogen and hydrides across the cladding wall (see Figures 1-3). During one-cycle drying at 400°C, cladding with >200 wppm hydrogen will have at most 200 wppm hydrogen below the hydride rim. The presence of circumferential hydrides in cladding at 400°C is an artifact of the pre-hydriding process that biases the precipitation of additional circumferential hydrides during cooling under stress and limits the number and length of radial hydrides that precipitate during cooling under stress. The hydride morphology in pre-hydrided cladding with >200 wppm hydrogen subjected to simulated drying conditions can result in significantly higher DBTT values relative to those for high-burnup cladding subjected to the same drying conditions. The effects of excess hydrogen across the cladding wall are shown in Figure 5. In previous Argonne work performed for the NRC, a pre-hydrided and pressurized rodlet (about 80 mm long) was fabricated from a ZIRLO™ segment with an axial variation in hydrogen content. It was exposed to the following simulated drying conditions: heated to 400°C, held for one hour at 400°C and 135-MPa hoop stress, slow cooled at 5°C/h from 400°C to 200°C under decreasing pressure and hoop stress conditions, and cooled more rapidly from 200°C to room temperature (RT). Rings sectioned from the rodlet were used for hydrogen-content measurements, metallographic examination, and ring compression testing. Figure 5a shows the hydride orientation for a ring with an average hydrogen content of 190 wppm. The radial-hydride continuity factor (RHCF) for this ring was essentially 100%. RHCF is a measure of the projection onto the cladding radius of continuous radial-circumferential hydrides within a 150-µm arc length. This projected length is then normalized to the wall thickness to determine a metric that correlates with depth of brittle cracking across the cladding wall in response to ring-compression loading. The ring shown in Figure 5a failed in a brittle manner during ring compression testing at 5 mm/s and 150°C. The second ring had an average hydrogen content of 250 wppm. The precipitated radial hydrides were relatively short and the RHCF was low. The ring was highly ductile (no cracking observed by visual inspection at low magnification) through 1.7-mm displacement at 5 mm/s and 150°C. Although visual low-magnification inspection revealed no cracking, micro-cracks may have developed along some of the short radial hydrides for this 250-wppm sample.

Based on the Argonne results, the NRC Division of Spent Fuel Storage and Transportation is currently NOT accepting data for non-irradiated, pre-hydrided cladding alloys to support license applications for high-burnup-fuel storage and transportation casks.

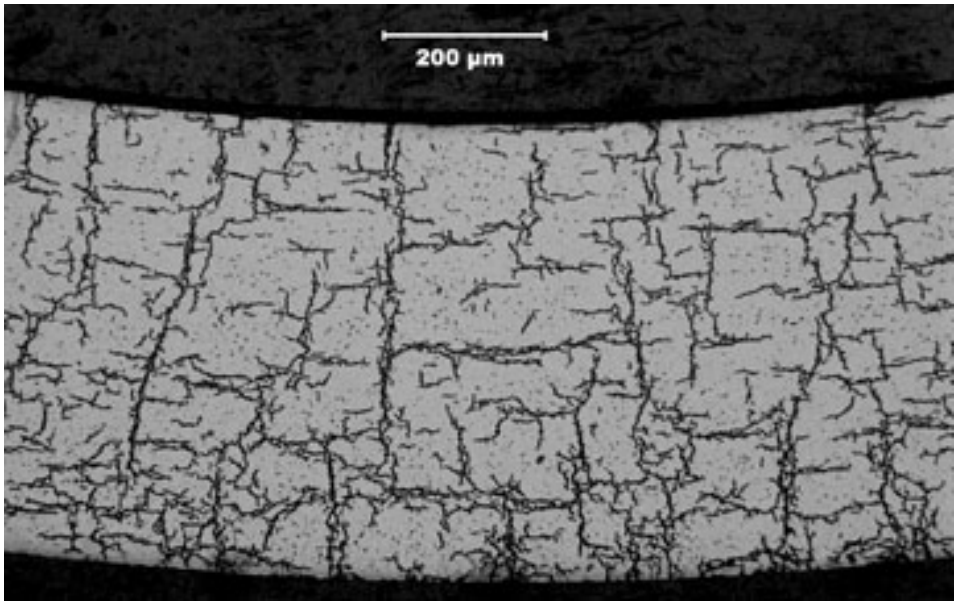

(a) 190 wppm H, brittle at 150°C

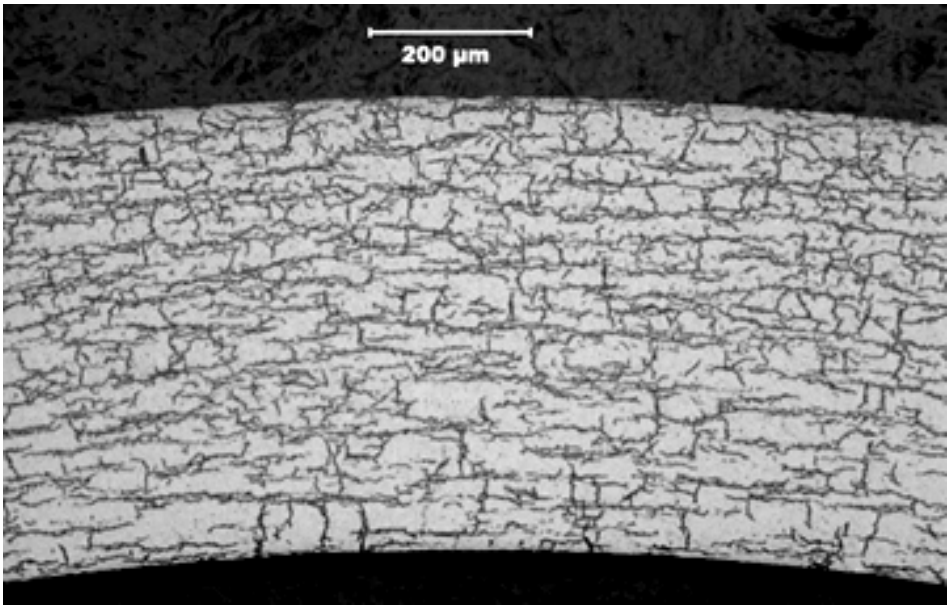

(b) 250 wppm H, ductile at 150°C

Figure 5. Hydrogen content and hydride morphology for non-irradiated, pre-hydrided ZIRLO™ rodlet that was pressurized and sealed prior to simulated drying at 400°C and 135-MPa hoop stress followed by cooling at 5°C/h under conditions of decreasing pressure and cladding hoop stress: (a) metallographic image for ring with 190 wppm hydrogen, which was brittle at 150°C under ring-compression loading; (b) metallographic image for ring with 250 wppm hydrogen, which was ductile at 150°C under ring-compression loading.

Aomi et al. (2008) studied the behavior of high-burnup Zry-2 (Zr-lined and RXA) and Zry-4 (CWSRA) following simulated drying at peak temperatures of 250-400°C and 250-340°C, respectively, and with cooling rates of 30°C/h, 3°C/h, and 0.6°C/h. Pressure and stress were held constant during cooling. Following simulated drying, ring compression tests (RCTs) and axial tension tests were performed at RT. They found that RXA Zry-2 was much more susceptible to radial-hydride formation and embrittlement than CWSRA Zry-4. At peak drying conditions of 400°C and 70-MPa hoop stress, they found long radial hydrides emanating from the Zry-2 outer surface and extending through more than 50% of the wall thickness. The results indicate that high-burnup Zry-2 needs to be included in the ring compression testing program (see Appendix). Also, the DBTT for high-burnup (<60 GWd/MTU) Zry-2 could not be determined as a function of drying conditions from the RT tests conducted by Aomi et al. With regard to their results for high-burnup (<56 GWd/MTU) Zry-4, the database was quite limited with respect to simulated drying temperatures (≤340°C).

Argonne performed five tests with high-burnup cladding for the NRC with simulated drying conducted at 400°C and 5°C/h cooling rate under decreasing pressure and hoop stress. The reference peak hoop stresses at 400°C were 140 MPa and 110 MPa. Results of the first two tests with high-burnup ZIRLO™ were documented and are publicly available through NRC ADAMS (Burtseva et al. 2010). Simulated drying for these two ZIRLO™ samples was conducted at 400°C hoop stresses of 140 MPa (see Figure 2 for approximate pre-test hydrogen content and hydride distribution) and 110 MPa (see Figure 3 for approximate pre-test hydride content and distribution). Results for the third test with high-burnup ZIRLO™ were documented, but they are not yet available to the public. The two tests with high-burnup Zry-4 samples were conducted at 400°C hoop stresses of 140 MPa (see Figure 1b for hydrogen content and hydride distribution) and 110 MPa (see Figure 1a for pre-test hydrogen content and hydride distribution). These results are scheduled to be documented in January 2012. In general, Argonne found that Nb-bearing ZIRLO™ was much more susceptible to radial-hydride formation and radial-hydride-induced embrittlement than Zry-4.

No data were found in the literature for radial-hydride formation and radial-hydride-induced embrittlement for high-burnup M5® cladding. As this alloy is both Nb-bearing and RXA, the expectation is that it will be susceptible to radial-hydride formation. However, radial-hydride-induced embrittlement may be partially mitigated by the low hydrogen content (≤100 wppm) typical of this alloy even after operation to high burnup.

2. APRIL 28, 2011 TEST PLAN

On April 28, 2011, Argonne issued its "Provisional Test Plan for High-Burnup Fuel Cladding and Modeling." Only PWR cladding alloys were included in the plan because cladding stresses in BWR Zry-2 were estimated to be too low (≤60 MPa) to cause radial-hydride embrittlement. Also, the emphasis was placed on testing high-burnup Zry-4 (4 pressurized rodlets for simulated drying and 16 RCTs) and ZIRLO™ (7 pressurized rodlets and 28 RCTs). This emphasis was based on Argonne tests conducted for the NRC. For high-burnup M5® one pressurized rodlet test was proposed for simulated drying at 400°C and 150 MPa peak drying conditions, which would be followed by four ring compression tests. The term "Provisional" refers to sequential testing in which the conditions for the next test with a cladding alloy are dependent on what was learned from the previous test with that alloy. If M5® exhibited ductility at RT (20°C) following drying at limiting temperature and hoop stress, then additional tests would not be needed. However, if test results indicated that the DBTT from the first M5® test was >20°C, then additional tests at lower drying stress and/or temperature would be conducted with varying simulated drying conditions until the DBTT criterion was met.

The Argonne test protocol used for NRC testing has been accepted by NRC for determining the conditions which lead to radial-hydride formation and radial-hydride-induced embrittlement. Thus, it is used in this test program to determine DBTT as a function of drying/transfer and early-stage storage temperatures and pressures. The test matrices in the April 28 plan are for (a) baseline characterization and mechanical property tests (axial tension and ring compression) of as-irradiated high-burnup cladding, and (b) test matrices for each high-burnup PWR alloy using both NRC limits on temperature and temperature cycling defined in ISG-11 (Rev. 3) and reduced temperature and temperature cycling limits. The ISG-11 (Rev. 3) limits are 400°C peak drying temperature, <10 thermal cycles during drying, and <65°C temperature drop per cycle. DBTT curves were to be determined at peak drying hoop stresses of 150 MPa, 110 MPa, and 70 MPa. If the resulting DBTT was found to be <20°C for an intermediate stress level, then testing would not be conducted at the lower stress level. The goal of subsequent testing was to determine if higher stresses (≥110 MPa) at lower drying temperatures would result in <20°C DBTT.

A revised test plan is needed to: a) clearly separate the two testing campaigns for NRC and DOE; b) include high-burnup Zry-2 on the basis of revised upper-bound stress level (120 MPa) and the results of Aomi et al. (2008); c) adjust peak drying stresses to 140 MPa, 110 MPa, and 80 MPa to be consistent with conditions used for NRC tests; and (d) expand the test matrix for M5® on the basis of the results presented in Section 3. Details of the revised Argonne test plan can be found in the Appendix.

3. HIGH-BURNUP M5® TEST RESULTS

3.1 Ring Compression Test and Apparatus Benchmarking

Ring compression tests are conducted with an Instron 8511 servohydraulic mechanical test system enclosed in a glove box. Figure 6a shows a schematic for the RCT. The tests are run in a displacement-controlled mode. The crosshead displacement rate is controlled to be constant and the displacement (δ) is measured as a function of time. The response load (P) is measured by a load cell in the static support component (6 o'clock position). Figure 6b shows a photograph of a cladding ring resting on the support plate with a small space between the loading plate and the top (12 o'clock) of the ring outer diameter. A clamshell radiant-heating furnace, which was opened for sample viewing purposes in Figure 6b, provides the heat for elevated temperature tests. Also, the three thermocouples, which contact the ring at the 3, 6, and 9 o'clock positions for elevated-temperature tests, were moved to the viewer's right for better imaging of the sample.

The Instron 8511 is calibrated annually with regard to load, displacement, and displacement rate measurements. However, before each high-burnup cladding test campaign, benchmark tests are conducted with as-fabricated cladding rings to ensure that the machine is operating properly and that load-displacement results are within expected values. The measured elastic loading stiffness (K_m) is compared to the calculated stiffness (K_c). For reference 8-mm-long rings, K_m is expected to be within 15% of K_c and generally less than K_c because of the influence of machine compliance. Following total displacement to $\leq$2 mm, the expected deviation between the offset displacement (δ_p) and the directly measured permanent displacement (d_p, difference between pre-test diameter and post-test diameter in the loading direction) is $\leq$0.2 mm, with $\delta_p > d_p$ because of the inherent error in using the offset-displacement methodology for RCTs.

Prior to conducting RCTs with high-burnup M5®, benchmark tests were conducted with as-fabricated 17×17 M5® rings with 9.48-mm outer diameter (D_o) and 0.63-mm wall thickness (h). The test conditions were chosen to be the same as would be used for the high-burnup cladding tests: 5-mm/s loading displacement rate, 1.7-mm total loading displacement, and 5-mm/s unloading displacement rate. All benchmark tests were conducted at RT. Figure 7 gives the load-displacement curves for benchmark Ring 1 (Figure 7a) and Ring 2 (Figure 7b). Ring 1 was 7.9 mm long and had a calculated loading stiffness of 1.18 kN/mm. Ring 2 was 7.7 mm long and had a calculated loading stiffness of 1.12-mm. As indicated in Figures 7a and 7b, the measured stiffness values for the two rings were 1.02 and 1.12 kN/mm, respectively. The average measured value was about 13% less than the calculated value, which is consistent with previous experience. From a ductility point of view, validation of the offset displacement (normalized to D_o to give relative strain) determined from the load-displacement curve is more important than validation of the loading stiffness. The offset displacement methodology calls for use of the loading slope to "unload" the sample after the loading phase. As can be seen from Figures 7a and 7b, δ_p and d_p are 1.19 mm and 1.05 mm, respectively, for both rings. The difference (δ_p - d_p) is 0.14 mm and is within the expected value based on a large database for as-fabricated cladding. The corresponding strains are calculated by normalizing the displacements to D_o: 12.6% offset strain and 11.1% permanent strain. The strain difference is 1.5%. Although permanent strain gives a more accurate value of plastic strain for rings that do not fail, it cannot be determined accurately for rings that crack prior to 1.7-mm total displacement. Based on assessments of error measurements and data trends, cladding with $\geq$1% permanent strain and

≥2% offset strain prior to the first crack extending through >50% of the wall is classified as ductile. Cladding that cracks through >50% of the wall prior to achieving 2% offset strain is classified as brittle.

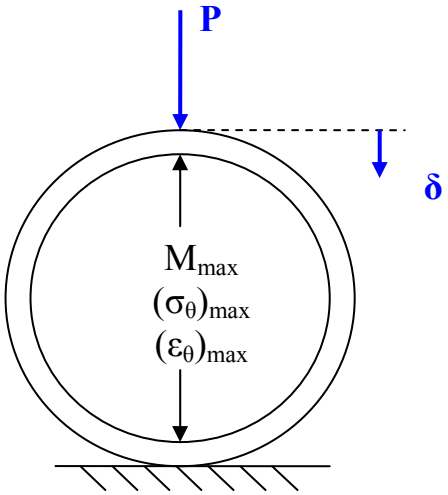

(a) Schematic of ring compression test

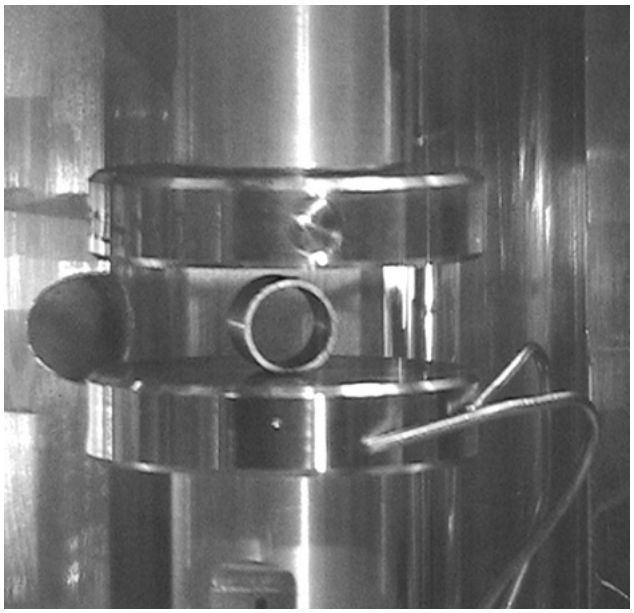

(b) Photograph of Instron 8511 with ring sample

Figure 6. Schematic (a) and photograph (b) of the ring compression test. The top plate (above the ring) is attached to the movable loading rod. The bottom plate (below the ring) is attached to the static support rod. Tests are conducted at a constant displacement (δ) rate. The resulting load (P) on the ring is measured by a load cell in the static bottom component. For imaging purposes in Figure 6b, the clamshell furnace used for elevated-temperature tests was opened and the thermocouples were moved to the right and below the ring.

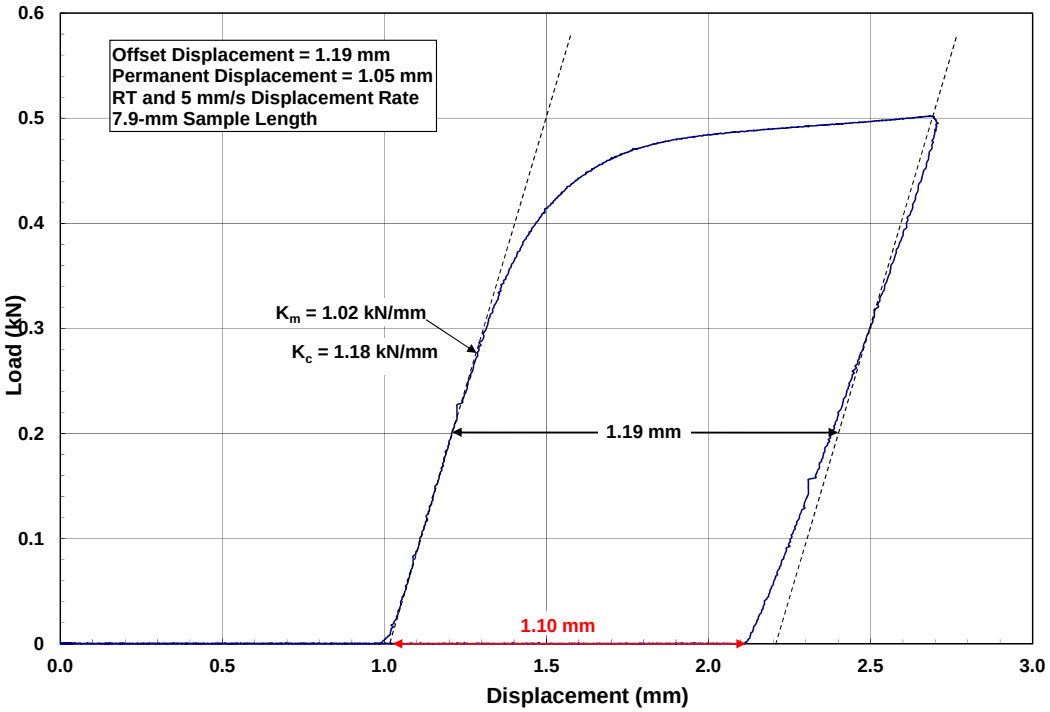

(a) Ring 1 (7.9-mm sample length)

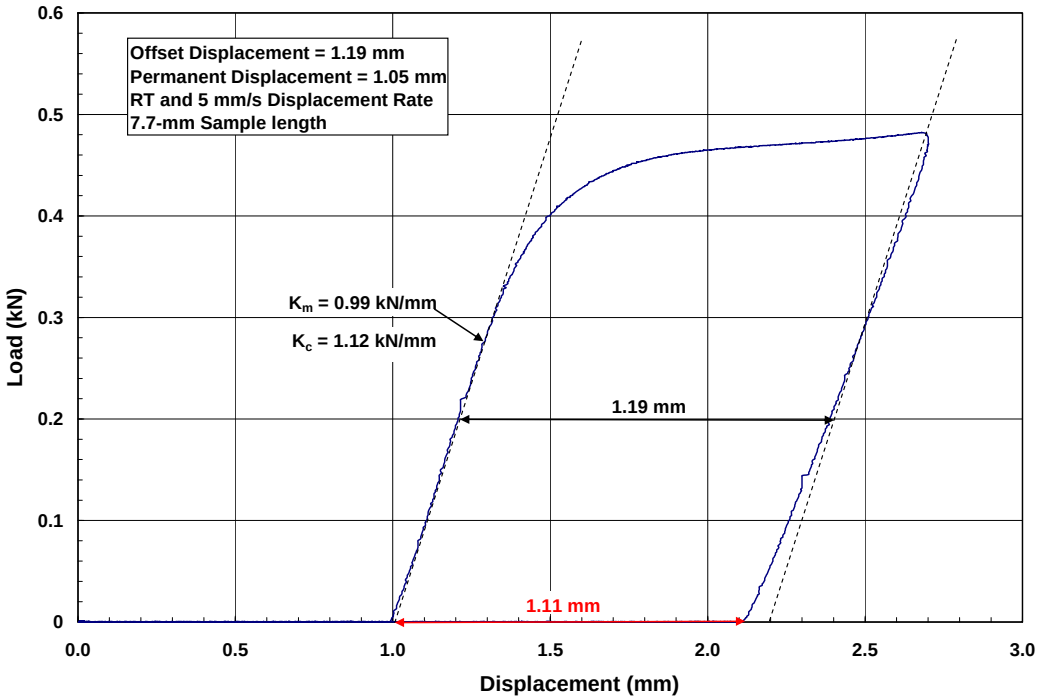

(b) Ring 2 (7.7-mm sample length)

Figure 7. Results of mechanical benchmark tests using the Instron 8511 machine to compress as-fabricated 17×17 M5® rings with 9.48-mm outer diameter and 0.63-mm wall thickness.

3.2 Results from First Test with High-Burnup M5®

For the first test, an 80-mm-long segment of defueled M5® cladding was selected from a fuel rod irradiated to 63 GWd/MTU. The axial location was 3.2 m from the bottom of the rod. However, the segment was within the uniform-burnup region of the rod and 0.1 m from the axial location at which the burnup began to decrease. Three segments within 2.8 to 3.2 m from the rod bottom were well characterized (see Figure 4) for the NRC LOCA program (Billone et al. 2008). On the basis of these characterization results, the expectation was that the corrosion layer would be about 12 μm thick and the hydrogen content would be about 100 wppm. The segment was pressurized and sealed to form a rodlet and the RT pressure was chosen to give 140-MPa hoop stress at 400°C. The rodlet was exposed to the reference simulated drying conditions for 17×17 cladding: temperature rise to 400°C, hold for 1 h at 400°C and corresponding pressure/stress, slow cool at 5°C/h to 200°C under decreasing pressure and hoop stress, and cool more rapidly from 200°C to RT.

Figure 8 shows the sectioning diagram for the rodlet following simulated drying. The measured hydrogen contents at four axial locations are labeled in the figure. The axial and circumferential variations in hydrogen content were relatively small. Measurements were made on four quarter-arc segments at each of four locations. The resulting 16 measurements were mass-averaged to give 94±6 wppm for the rodlet, in good agreement with the 100-wppm sibling data reported in Fig. 4. On the basis of metallographic images for ring 7, the corrosion layer was 13 μm thick, the cladding metal was 0.55 mm thick, >95% of the hydrides were in the radial direction, and the RHCF was 51±14%. The cladding metal outer diameter was 9.43 mm.

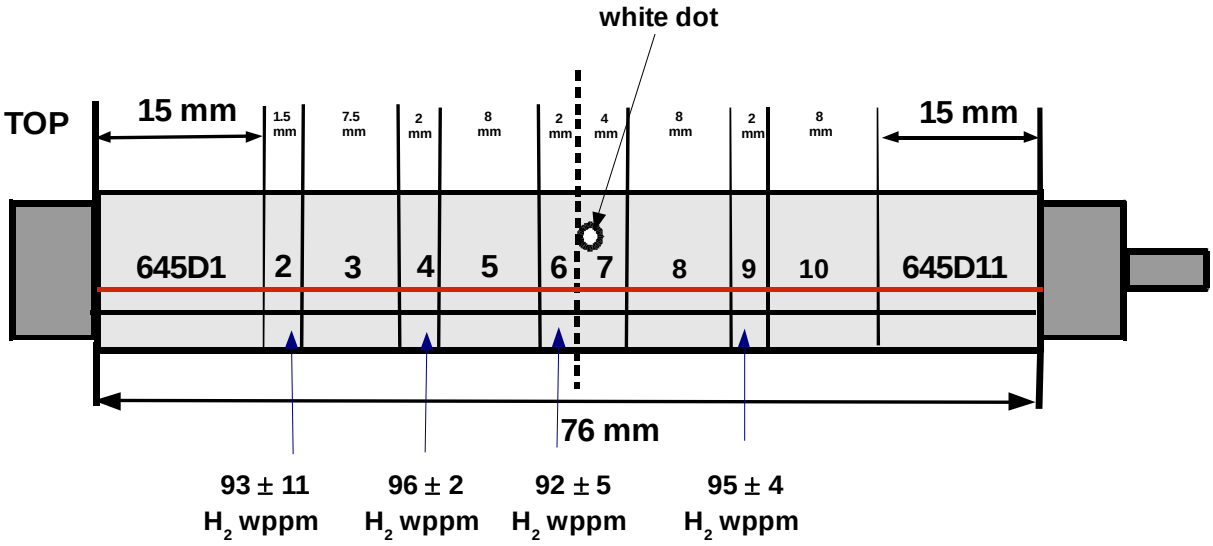

Figure 8. Sectioning diagram for M5® segment (645D) after simulated drying of the pressurized and sealed rodlet. Rings 2, 4, 6, and 9 were used for hydrogen-content measurement. Ring 7 was used for metallographic imaging (white dot indicates surface imaged). Rings 3, 5, 8 and 10 were used for ring compression tests.

Ring compression tests (RCTs) were conducted at a 5-mm/s loading displacement rate to 1.7-mm total displacement and at a 5-mm/s unloading displacement rate. RCT temperatures were varied from 30°C to 150°C to allow determination of the DBTT. The testing sequence was: 150°C (ring 5), 30°C (ring 8), 90°C (ring 10) and 60°C (ring 3). Offset strains were determined from the load-displacement curves and permanent strains were determined from diameter measurements. Offset strains were 0.7%, 0%, 6.8%, and 11.6% for test temperatures of 30°C, 60°C, 90°C and 150°C, respectively. The DBTT was estimated to be 80°C.

Load-displacement curves for the 4 rings are shown in Figures 9-12. The failure criterion used was >50% wall cracking, which corresponds to >50% decrease in loading slope during elastic deformation or >22% steep load drop during plastic deformation. The results for the 150°C ring that did not crack were used to develop a correction correlation for offset strain based on the decrease in unloading slope (K_{Um}) relative to the loading slope (K_{Lm}).

Visual inspection of ring 8 tested at 30°C indicated through-wall cracks at the 12 and 6 o'clock positions and a 90% wall crack at about the 8 o'clock position. Visual inspection of ring 5 tested at 150°C indicated no cracking. Both visual and metallographic examinations were performed for ring 3 tested at 60°C and ring 10 tested at 90°C. Visual examination of the ends of ring 3, tested at 60°C, indicated though-wall cracks at the 12 and 6 o'clock positions and partial-wall cracks at the 3 and 9 o'clock positions. Based on metallographic imaging, the RHCF for ring 3 was 67±20% and the observed cracks were: 74% at 12 o'clock, 88% at 3 o'clock, 100% at 6 o'clock, and 96% at 9 o'clock. Visual examination of the ends of ring 10 tested at 90°C indicated 70-80% wall cracks at the 12 o'clock position and 15-25% wall cracks at the 6 o'clock position. On the basis of metallographic imaging of a cross section at the mid-span of ring 10, the RHCF was 67±13%. A single 60% wall crack was observed at the 12 o'clock position with a short parallel crack extending an additional 15% into the wall. The metallographic results for the ring tested at 90°C support the conclusion that the ring had significant ductility (about 7%) prior to cracking. Based on images for the three metallographic samples, the average value for RHCF was 61±18% for the high-burnup M5® rodlet subjected to peak simulated drying conditions of 400°C and 140-MPa hoop stress.

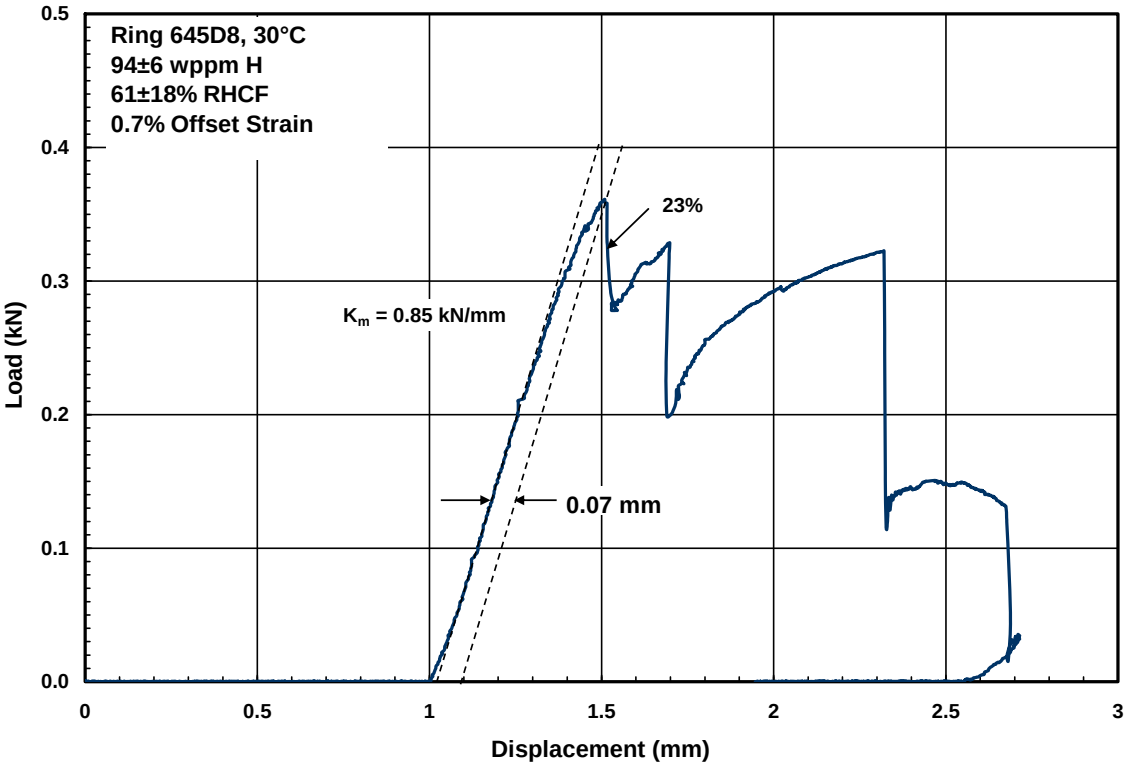

Figure 9. Load-displacement curve for ring 8 tested at 30°C and 5-mm/s displacement rate.

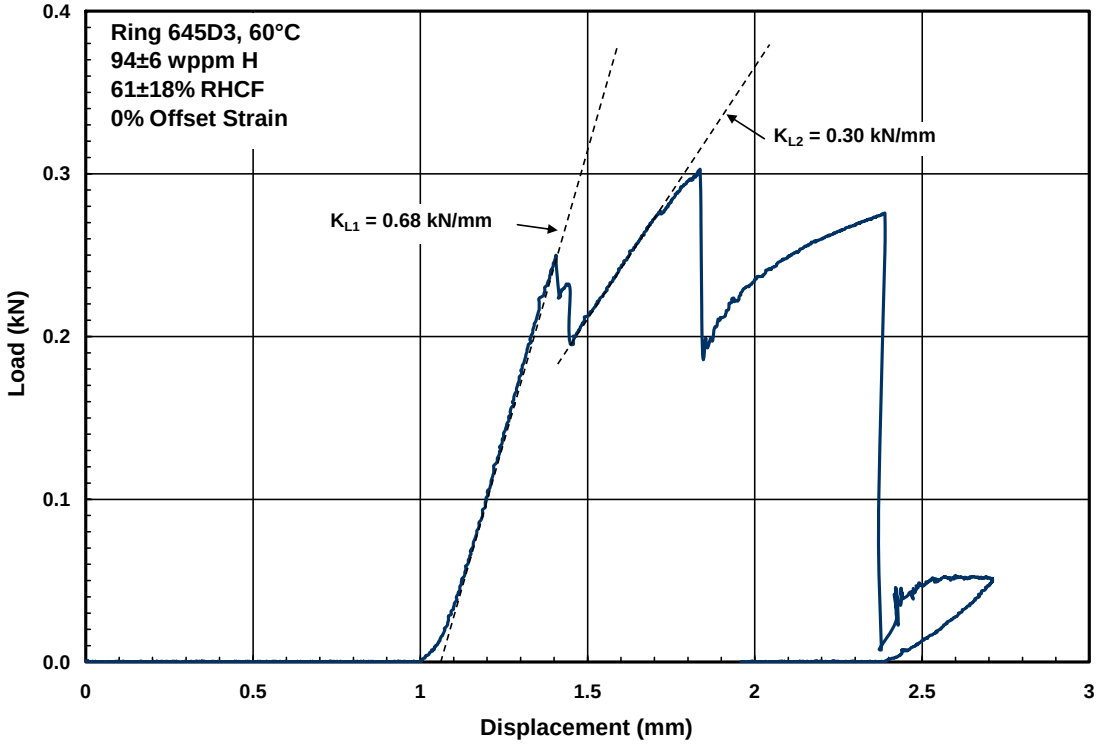

Figure 10. Load-displacement curve for ring 3 tested at 60°C and 5-mm/s displacement rate.

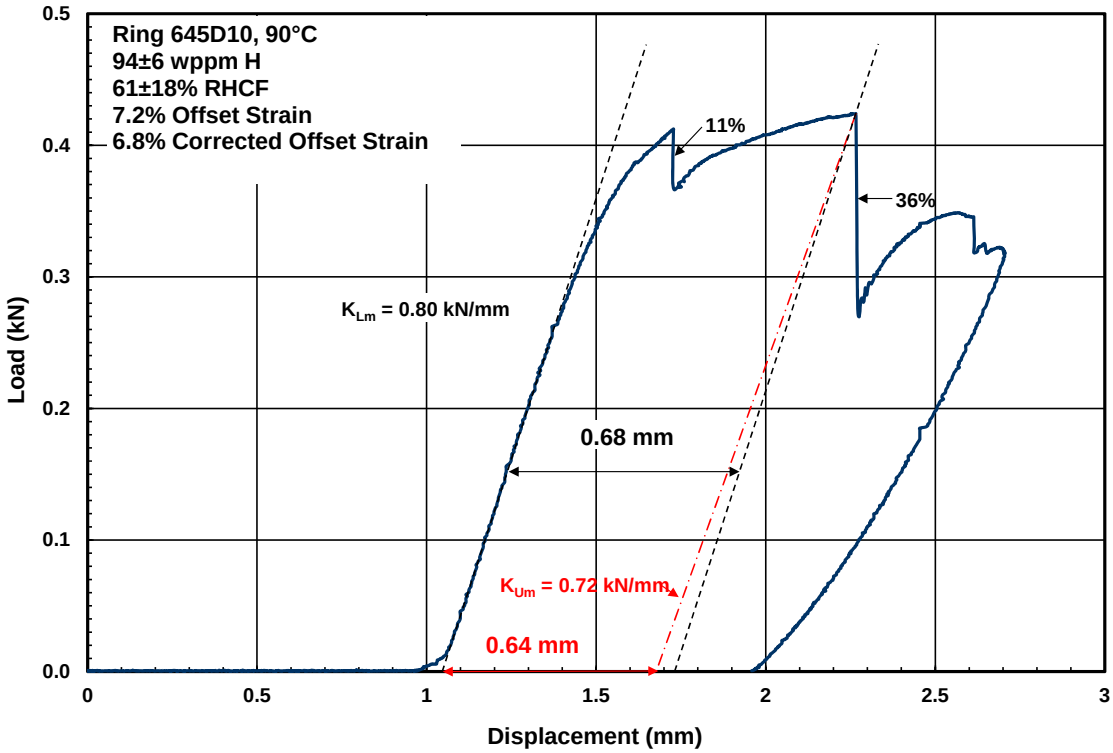

Figure 11. Load-displacement curve for ring 10 tested at 90°C and 5-mm/s displacement rate.

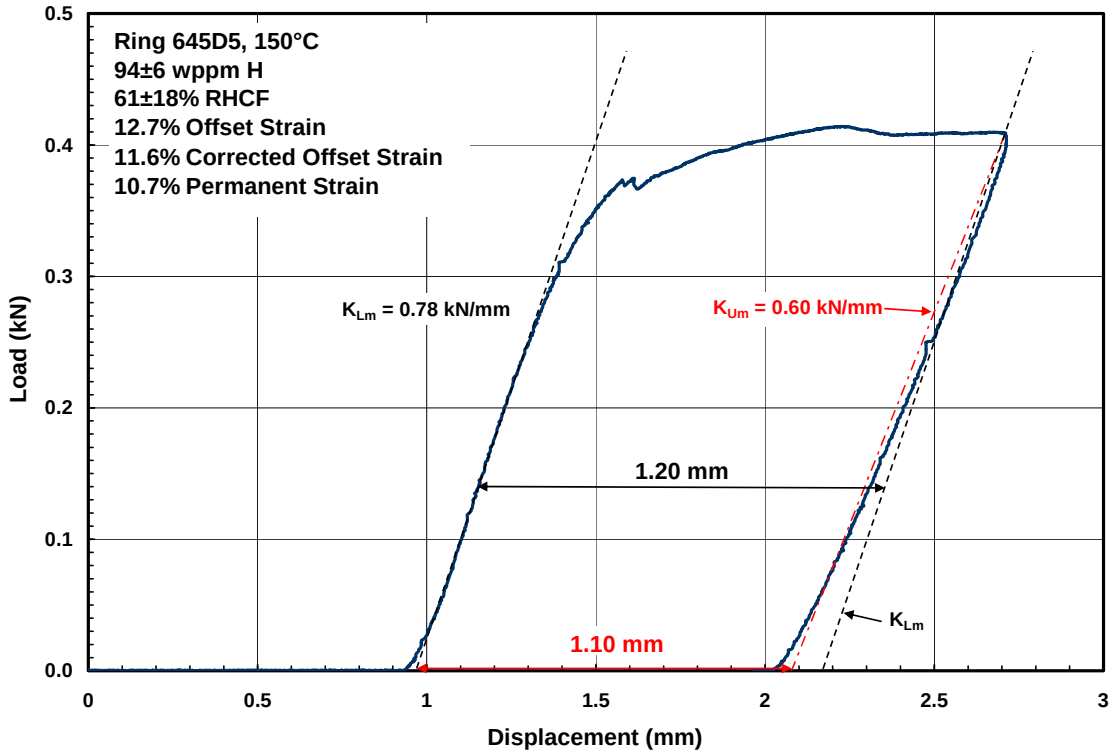

Figure 12. Load-displacement curve for ring 5 tested at 150°C and 5-mm/s displacement rate.

3.3 Results from Second Test with High-Burnup M5®

As the DBTT (80°C) for the first high-burnup M5® rodlet was >20°C, a second test was conducted at a reduced 400°C hoop stress of 110 MPa to determine if the lower drying stress would result in a lower DBTT. A 76-mm-long segment from another M5®-clad fuel rod irradiated to 68 GWd/MTU was used to fabricate the sealed and pressurized rodlet (651E5). As the hydrogen content was anticipated to be lower for this segment, the slow cooling at 5°C/h was extended to 130°C to allow most of the hydrogen to precipitate at this slow cooling rate. Following this simulated drying-storage thermal history, characterization and ring compression testing were conducted. Figure 13 shows the sectioning diagram for the rodlet following simulated drying. Characterization results for a cross section near the middle of the rodlet (ring D) were: 8 µm corrosion-layer thickness, 0.56 mm metal wall thickness, 72±10 wppm hydrogen content, and 33±7% RHCF. The outer diameter of the cladding metal was 9.51 mm.

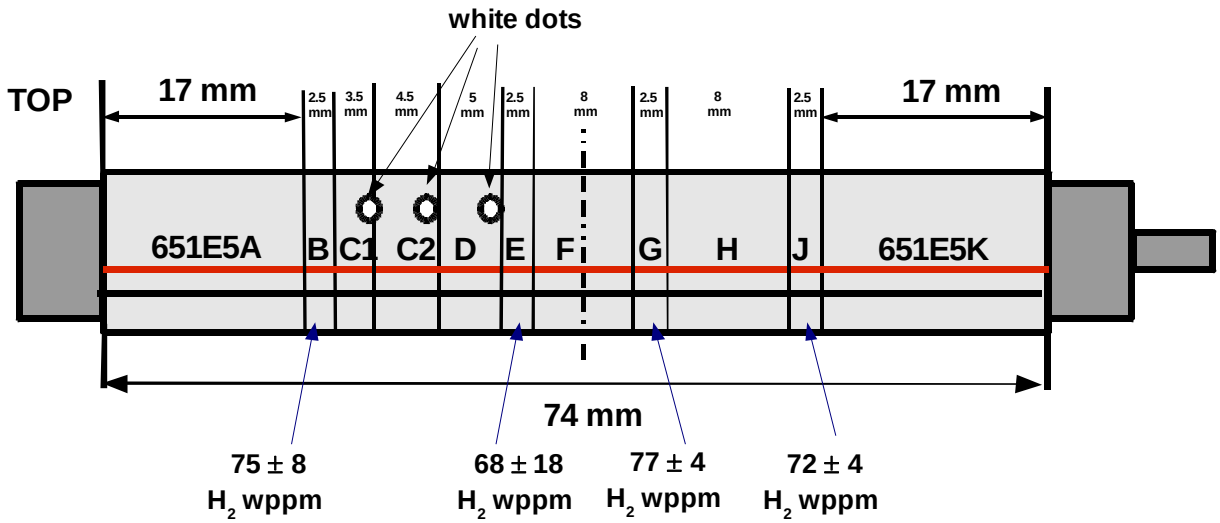

Figure 13. Sectioning diagram for M5® segment (651E5) after simulated drying of the pressurized and sealed rodlet. Rings B, E, G, and J were used for hydrogen-content measurement, as indicated. Ring D was used for metallographic imaging (see white dot, which indicates surface imaged). Rings C, F, and H were used for ring compression tests. Following ring compression testing of ring C, it was sectioned to generate two samples for metallographic imaging.

The rings tested at 30°C and 60°C were brittle and the ring tested at 90°C was highly ductile (no cracking through 1.7-mm displacement and about 11% offset strain). The estimated DBTT was 70°C. Figures 14-16 show the load-displacement curves for ring H tested at 30°C, ring C tested at 60°C, and ring F tested at 90°C. The corresponding offset strains were 1.4%, 1.1%, and 11% (corrected value).

Visual and metallographic examinations were performed for the 651E5 ring (C) tested at 60°C. The load-displacement curve for this ring indicated a steep load drop of 27% at 0.6 mm total displacement, which corresponded to an offset strain of about 1%. Based on Argonne's large database for compressed rings, the steep 27% load drop is indicative of unstable crack growth through more than 50% of the cladding wall thickness and the 1% offset strain is within the uncertainty range for ductility determination. Offset strains need to be ≥2% prior to >50% wall cracking for the material to be classified as ductile. Visual observation of the ends of the ring indicated cracks extending through about 100% of the wall at the 12

o'clock position (under the applied load) and a crack at 6 o'clock (above the support) that extended through about 80% of the wall on one end (Side 1) and was nonexistent on the other end (Side 2). Metallography samples were prepared to image (at 25X, 100X, and 200X) the ring C mid-span Side 2 cross sections. Cracks imaged at the mid-span have the following lengths: 100% of the wall (i.e., through-wall) at the 12 o'clock position and 70% of the wall at the 6 o'clock position. The RHCF for this mid-span cross section was measured to be 64±20% based on images taken at 13 angular orientations. For Side 2 (after grinding, polishing and etching), only one crack was observed: 50% through-wall at the 12 o'clock position. The RHCF for this cross section was measured to be 57±16% based on images at 14 angular orientations. Overall, based on the images taken at three axial locations about 5 mm apart, the RHCF for rodlet 651E5 was 54±20%.

Important conclusions that can be drawn from the two high-burnup M5® tests are: (a) lowering the peak drying stress from 140 MPa to 110 MPa had a relatively small effect on radial hydride formation and consequently DBTT (decreased from 80°C to 70°C); (b) there is significant variation in effective radial hydride length (i.e., RHCF) in both the circumferential and axial directions; and (c) the extent of wall cracking varies along the axis of the compressed ring. Figure 17 shows the ductility vs. test temperature results from the two tests. It is clear that the next test should be conducted at a peak drying stress of 80 MPa at 400°C to determine if that has a significant effect on lowering the DBTT from 70°C to 20°C.

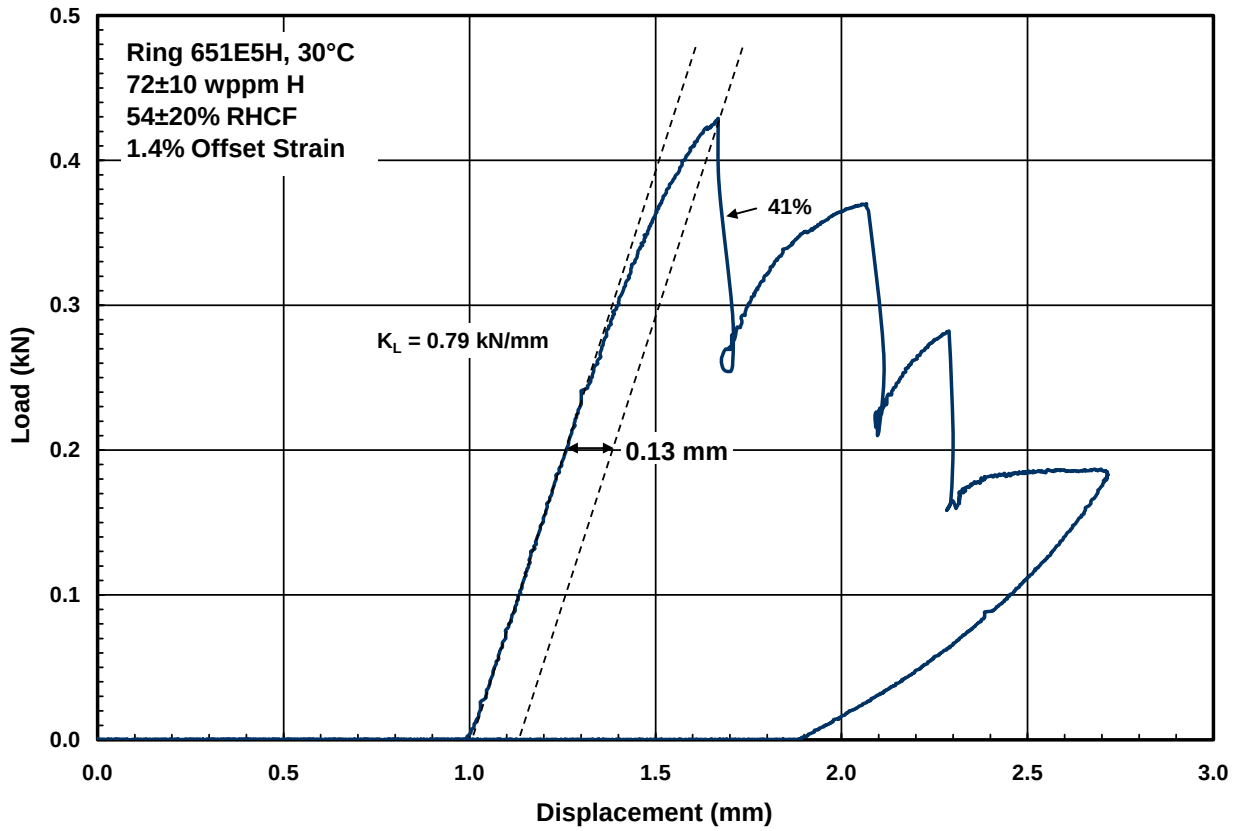

Figure 14. Load-displacement curve for ring H tested at 30°C and 5-mm/s displacement rate.

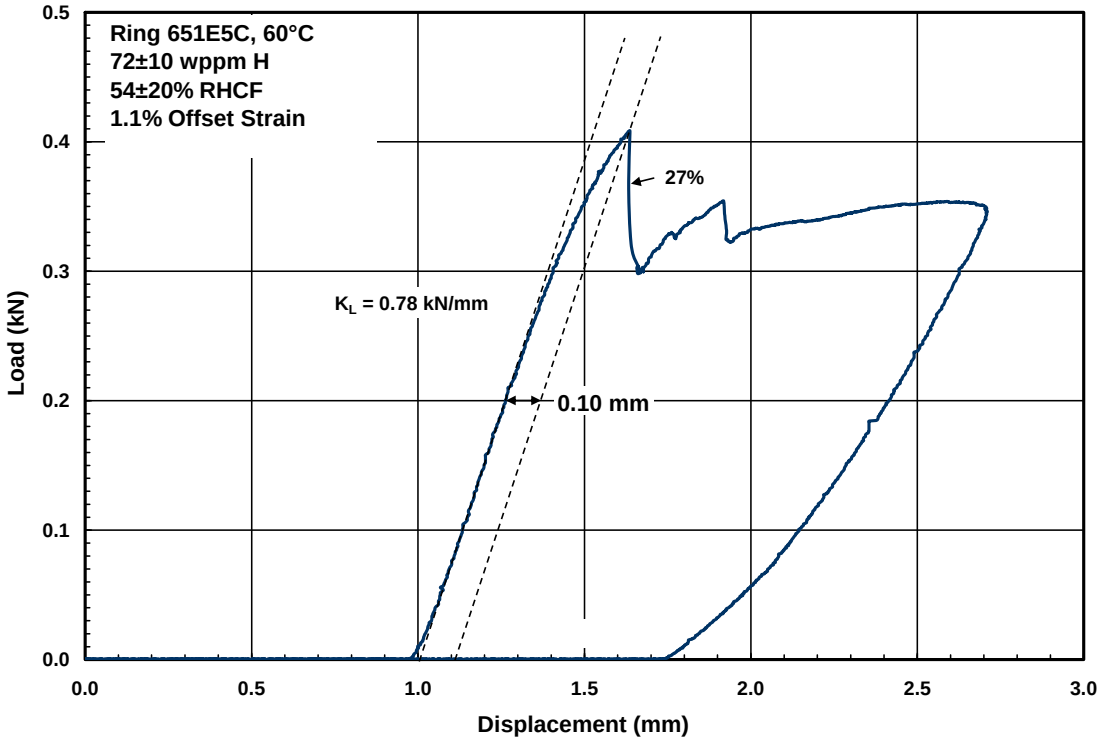

Figure 15. Load-displacement curve for ring C tested at 60°C and 5-mm/s displacement rate.

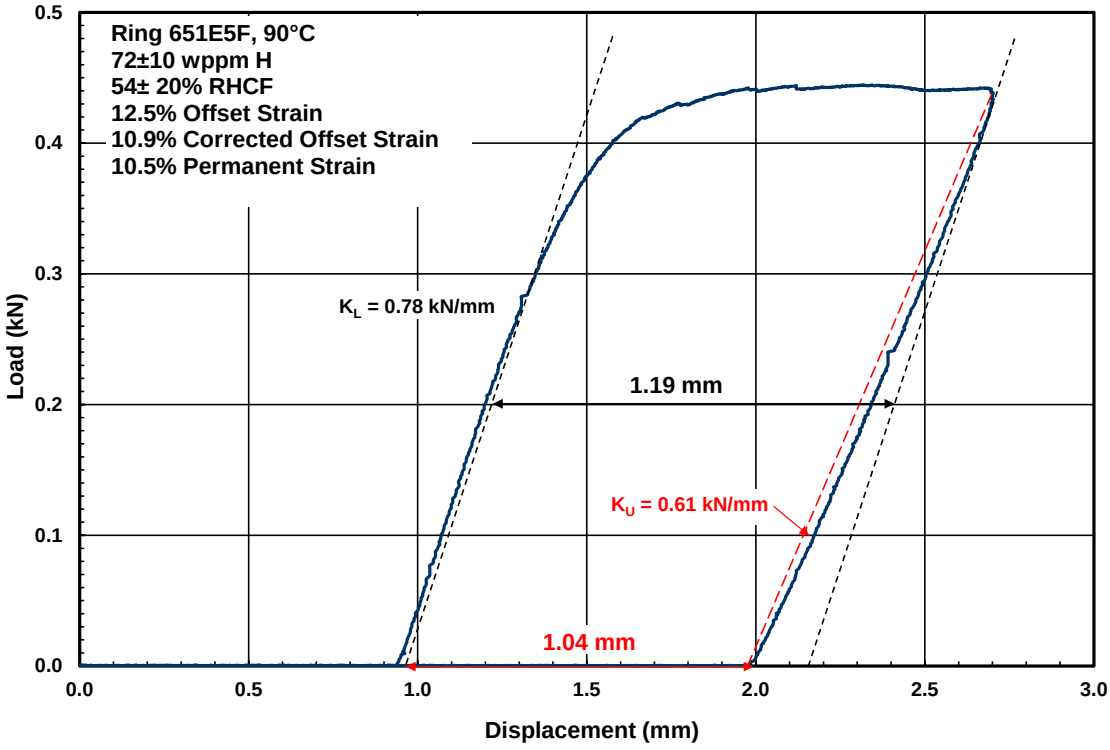

Figure 16. Load-displacement curve for ring F tested at 90°C and 5-mm/s displacement rate.

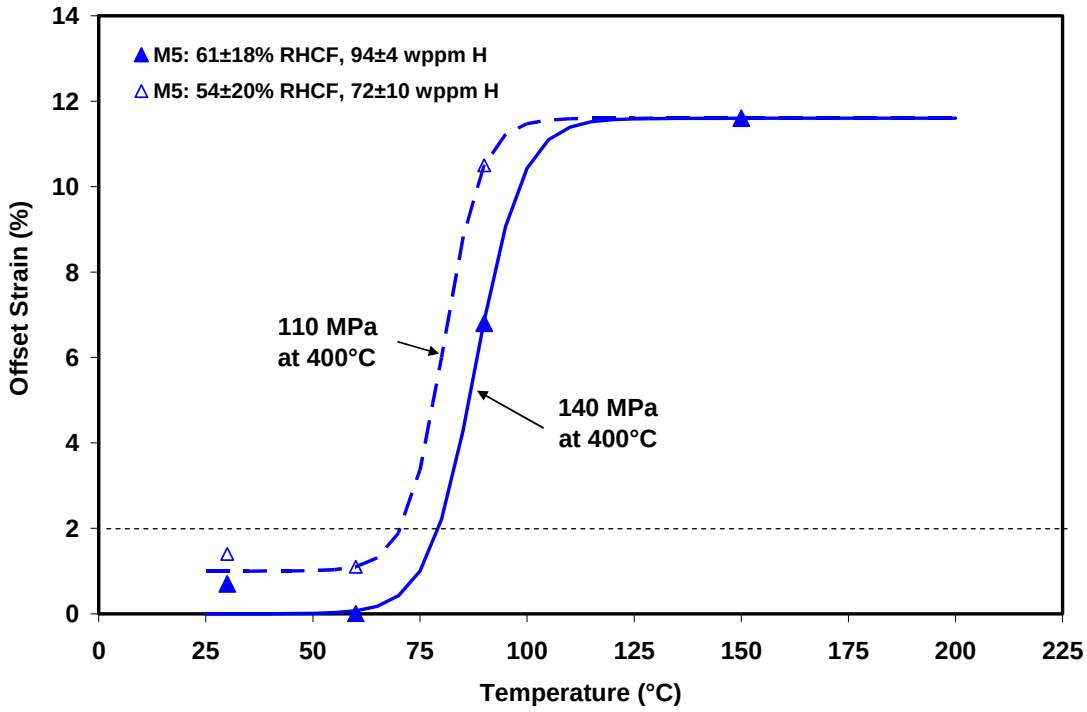

Figure 17. Ductile-to-brittle transition temperature (DBTT) curves for high-burnup M5® cladding following simulated drying at 400°C peak temperature and 400°C hoop stresses of 140 and 110 MPa. Offset strain is a measure of plastic strain. Offset strain values <2% are within the uncertainty of the measurement. Hence, rings with <2% offset strain are classified as brittle.

4. REVISIONS TO THE ARGONNE TEST PLAN

4.1 Baseline Studies

These tests remain basically the same as the ones proposed in the April 28 test plan with the exception of adding high-burnup Zry-2 to the test matrices that were designed for high-burnup PWR alloys Zry-4, ZIRLO™, and M5®. The Zry-2 of interest is from fuel rods irradiated in one of the Limerick reactors to 65 GWd/MTU. One segment of each alloy will be used to run two axial tensile tests per alloy at RT and two strain rates (e.g., 0.1%/s and 100%/s). If the cladding alloys show little strain-rate sensitivity, no further axial tensile tests will be required. For any alloy that shows significant strain-rate sensitivity, a third test will be conducted at >100%/s strain rate. The results of these studies will be used to determine mechanical properties (i.e., yield and ultimate strength and uniform and total elongation) of as-irradiated cladding prior to its transfer from the pool, drying, transfer and dry-cask storage.

Also included in the baseline studies of as-irradiated cladding are characterization and RT ring compression testing at 3 displacement rates (0.05 mm/s, 5 mm/s, and 50 mm/s). Characterization will include metallographic examination and hydrogen determination at both ends of the ≈8-cm-long segments. Corrosion-layer thickness, metal wall thickness, hydride distribution across the cladding radius, and hydrogen content will be determined. For cladding alloys with a thick outer-surface oxide layer and hydride rim (i.e., Zry-4 and ZIRLO™), additional metallography and hydrogen content measurements will be performed with the corrosion layer removed and with the corrosion layer and hydride rim removed. Work that is currently in progress as part of these baseline studies is shown in Figure 18 for a high-burnup Zry-4 segment with a corrosion layer of ≈ 100 μm and a hydrogen content of ≈700 wppm.

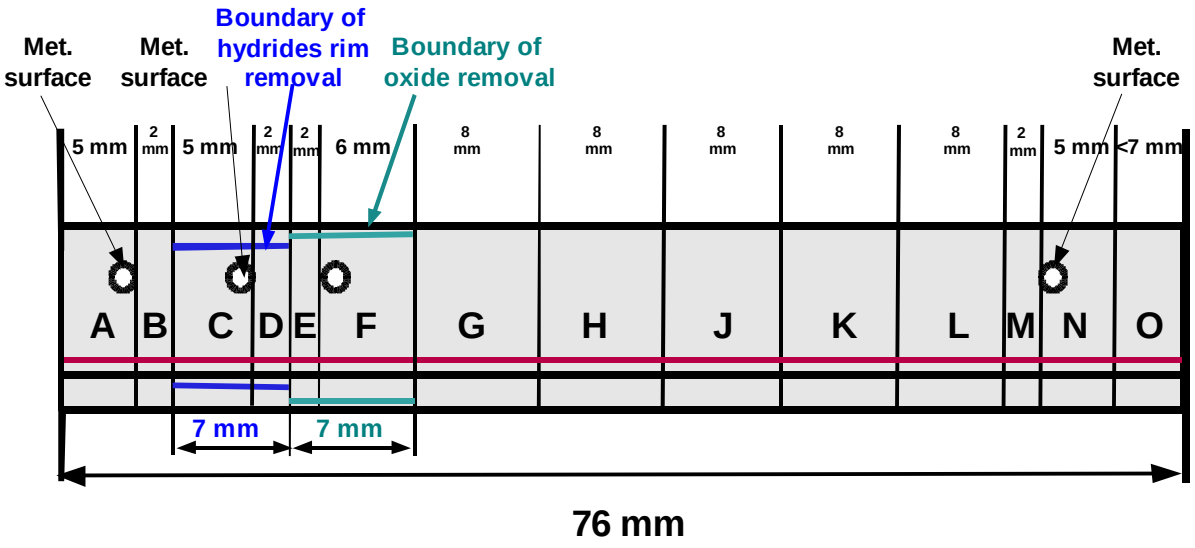

Figure 18. Sectioning diagram for baseline characterization and ring compression testing of a high-burnup Zry-4 cladding segment. Rings A, C, F, and N are metallographic samples with the white dots indicating the surfaces to be imaged. Rings B, D, E and M are for hydrogen content determination. Rings G-L are for ring compression testing.

4.2 Testing at ISG-11 (Rev. 3) Limits

Ring compression tests (RCTs) will be performed on high-burnup cladding samples subjected to drying/transfer-storage limits established by the NRC in ISG-11 (Rev. 3). These limits are 400°C peak cladding temperature, <10 cooling cycles, and <65°C temperature drop per cooling cycle. Based on cask-vendor/utility experience with vacuum drying, only 3 to 5 cooling cycles would be needed. Also, a practical time interval between cooling cycles is about 24 hours. During this interval the temperature drop would be >65°C. Thus testing will be conducted for 1, 3 and 5 drying cycles with 100°C temperature drop per cycle.

The matrices for these tests (see Appendix) incorporated the experience from testing high-burnup Zry-4 and ZIRLO™ (Burtseva et al. 2010) for NRC, and high-burnup M5® for DOE since July 2011. High-burnup Zry-4 retains ductility at 20°C following 1-cycle simulated drying at a 400°C hoop stress of 110 MPa. To complete testing for this alloy at ISG-11 (Rev. 3) limits, additional tests will be conducted on samples subjected to 3- and 5-cycle temperature drops from 400°C to 300°C with a peak hoop stress of 110 MPa. Also, it is clear from the work performed for NRC that the peak hoop stresses for high-burnup ZIRLO™ have to be <110 MPa to achieve a DBTT <20°C. The next tests with ZIRLO™ will be conducted at a 400°C hoop stress of 80 MPa and 1, 3 and 5 temperature cycles with 3- and 5-cycle temperature drops from 400°C to 300°C. The 80-MPa hoop stress is of particular significance to the guidance in ISG-11 (Rev. 3) as the guidance implies that radial-hydride embrittlement does not occur at hoop stresses <90 MPa based on data primarily for non-irradiated, pre-hydrided Zry-4. The stress threshold may not be valid for high-burnup cladding alloys, especially ZIRLO™, M5® and Zry-2. For high-burnup M5®, the 400°C hoop stress will also be reduced to 80 MPa. If there is a mixture of radial and circumferential hydrides under this simulated drying condition, then temperature cycling may be introduced. For high-burnup Zry-2, which is not currently available at Argonne, testing will be initiated at a 400°C hoop stress of 120 MPa. This stress will be reduced to 90 MPa and 60 MPa, if needed, to achieve <20°C DBTT, or to at least minimize the DBTT. The results of these tests will be used to determine the 400°C hoop-stress level at which temperature cycling will be introduced.

The results of these tests will be a set of DBTT curves (offset strain vs. test temperature) for each set of simulated drying conditions at ISG-11 (Rev. 3) limits and for each high-burnup cladding alloy.

4.3 Testing at Less than ISG-11 (Rev. 3) Limits

In this set of tests, the peak temperature limit of 400°C will be reduced to determine if higher stresses can maintain <20°C DBTT or at least minimize DBTT to the same levels determined in Section 4.2 testing. Tests will first be conducted at a peak drying temperature of 350°C to determine the benefit with regard to peak hoop stress at that temperature. The stress levels used in these tests will depend on the results of the Section 4.2 tests. If a significant increase (e.g., 30 MPa) in allowable stress results from this decrease in peak drying temperature, a second set of tests may be conducted at 325°C. Drying temperatures <300°C can be achieved with forced helium-flow dehydration. However, peak temperatures lower than 325°C may be too restrictive with regard to cask loading and heating rate. Both non-irradiated, pre-hydrided and high-burnup cladding will be used in testing at less than the ISG-11 (Rev.3) limits. Test matrices will be similar to those shown in Tables 4 and 5 of the Appendix, except that the peak drying temperature will be reduced and the peak drying stress will be increased.

Although the goal of the ring compression testing is to determine drying/transfer-storage conditions for which DBTT is <20°C, this goal may not be achievable for all cladding alloys at peak temperatures and stresses that are acceptable and/or practical. Regardless of whether this goal can be achieved, the data generated for DBTT vs. drying conditions will allow informed trade-offs between drying/transfer-storage conditions and post-storage retrieval and transportation temperatures.

4.4 Modeling

Cladding materials modeling and canister/cask modeling will be conducted in parallel with the test program and utilize the mechanical test data as input as well as for benchmark verification. Materials modeling will include the following: (a) precipitation temperature of hydrides during cooling under stress; (b) stress-strain behavior under hoop bending loading of the composite cladding material containing brittle hydrides in a low-ductility matrix; (c) correlation between measured ductility (δ_p/D_o) of the cladding and the local plastic deformation in cladding prior to and after developing wall cracks; (d) correlation between change of cladding stiffness slope and crack depth into the cladding for rings that crack during the linear cladding deformation mode; (e) correlation between magnitude of steep load drop during elastic-plastic deformation and crack depth into the cladding wall (i.e., crack depth as a fraction of cladding wall thickness vs. percentage of load drop); and (f) condition of cladding with a 50% wall crack in response to pressure-induced hoop stress and axial bend stresses. The background for item (b) is documented by Billone (2011). Billone showed that within the elastic deformation regime, the elastic strain calculated by δ_p/D_o is three times the maximum elastic strain (ε_e) in the cladding material. While δ_p/D_o (with <2% strain indicating brittle behavior) is a useful metric using the RCT as a ductility screening test, it does not represent the local ductility in the cladding.

With regard to canister/cask modeling, this activity will be coordinated with colleagues at other DOE laboratories developing canister/cask thermal and mechanical models. Radial-hydride formation is highly dependent on fuel rod internal pressure, peak cladding temperature, and axial distribution of cladding temperature during drying and early stages of storage. If such modeling calculations are not provided, Argonne will use existing codes, such as ANSYS and FLUENT, to perform thermal calculations to estimate the peak cladding temperatures of used fuel assemblies within a canister or cask during drying/transfer and early dry-cask storage. Argonne will also use existing codes, such as ABAQUS and LS-DYNA, to perform structural calculations to evaluate the mechanical response of used fuel assemblies during drops of a canister/cask under normal conditions of transport and hypothetical accidents, employing mechanical properties data and correlations determined from the cladding testing program and material modeling.

4.5 Recent Meetings

During the first quarter of fiscal year 2012, Argonne staff attended the following meetings that are related to testing of high-burnup fuel cladding:

1) NRC Technical Exchange and Regulatory Conference, Washington, D.C., November 1-2, 2011, during which a panel discussion was held on high-burnup fuel and on the alternatives for addressing criticality safety requirements for high-burnup fuel transportation. Einziger (2011) presented the

progress and results of NRC's cladding programs and discussed cladding mechanical properties that depend on alloy type, mechanical treatment, irradiation, drying procedure, and temperature range of use. Einziger also discussed the hydride reorientation phenomenon, its importance, and the current state of knowledge. With regard to the objective of the NRC test program, he stated "Determine if the cladding has residual ductility after cooling slowly under a deceasing stress commensurate with a decreasing temperature as would be experienced during and after vacuum drying." With regard to test methodology, he referenced the Argonne RCTs of radial-hydride-treated high-burnup cladding as "Protocol established to determine ductile to brittle transition after hydride reorientation." With regard to future work, Einziger stated that NRC plans to publish the results of the Argonne testing (supported by NRC up through the early part of fiscal year 2011) in the spring of 2012; on the basis of these results, NRC will either revise ISG-11 (Rev. 3) or issue a new ISG detailing guidance on properties to use for high-burnup cladding and suggested protocol to establish properties under different conditions or for different alloys, while continuing to survey new results for influence on guidance. NRC also expects industry to provide test data for different alloys, as needed, and/or stress and temperature conditions to justify use of materials properties and to provide better lower-temperature distributions. The Argonne ring compression testing methodology is thus accepted by NRC as a protocol to generate data to support the development of the technical basis and guidance for licensing storage and transportation of high-burnup fuel. The UFDC Phase I tests and subsequent ring compression tests of different high-burnup cladding alloys are designed to generate new results that could be used for guidance, while providing industry with the test data needed for different cladding alloys.

2) DOE UFDC Meeting on Test and Validation Complex, Washington, D.C., November 3, 2011, during which discussions were held on the development of a comprehensive plan to address the technical, logistical, and operational aspects of conducting the near-term separate effects tests and the longer term demonstration project. The ST Test and Evaluation Capabilities Development control account has been re-scoped in December 2011 to "Field Testing," with guidance provided to each Laboratory on the new scope, activities and milestones for the remainder of fiscal year 2012.

3) DOE Fuel Cycle Technology Annual Review, Argonne, IL, November 8-10, 2011, during which Sorenson presented a review of used-fuel disposition storage and transportation activities. Argonne staff conducted a tour of the Irradiated Materials Laboratory for Kemal Pasamehmetoglu, et al. and described the experimental capabilities for steam oxidation of irradiated Zircaloy cladding, and the work conducted for NRC on cladding behavior during simulated loss-of-coolant accident conditions.

4) DOE UFDC Cladding Test Plan Workshop, Las Vegas, NV, November 15-17, 2011, during which Argonne made three presentations on "High-burnup Fuel Issues (Liu and Billone)," "Cladding Test Methods and Data (Billone)," and "ANL Test Plan for High-Burnup Fuel Cladding Behavior (Billone and Liu)." These presentations covered the background and history of high-burnup fuel issues, cladding testing methods, the Argonne ring compression testing methodology developed for NRC and employed in the current DOE testing of high-burnup fuel cladding, as well as highlights of the results from the Phase I testing of high-burnup M5®, and the essence of the revised Argonne test plan for continuing ring compression testing of high-burnup fuel cladding in 2012 and beyond. The high-burnup fuel issues and data needs are also discussed in a paper (by Billone et al.) titled "High Burnup Fuel Issues for Long-Term Dry Cask Storage and Transportation." The paper was peer reviewed and accepted by the 14th International Conference on Environmental Remediation and Waste Management (ICEM), Reims, France, September 25-29, 2011. Per NRC's request, the paper was not

presented at ICEM 2011; it was distributed within the DOE community because the work was funded by UFDC in fiscal year 2011.

5) EPRI Extended Storage Collaboration Program (ESCP) Meeting, Charlotte, NC, December 4-5, 2011, during which John Kessler, Chairman of the ESCP, gave a review of the gap analyses conducted by the Nuclear Waste Technical Review Board, DOE and NRC up to August 2011 (Kessler 2011). Compared to the three major R&D gaps identified by the ESCP in December 2010, which included condition of used fuel at the time of transport, the importance of R&D on cladding hydride reorientation has been ranked "high" by DOE (draft), "medium" by NRC (draft), and "medium" by EPRI (final); the difference arose primarily over fuel retrievability, i.e., whether it is required for transportation after storage. However, 10 CFR 72.122 (h)(5) states "The high-level radioactive waste and reactor-related GTCC waste must be packaged in a manner that allows handling and retrievability without the release of radioactive materials to the environment or radiation exposures in excess of part 20 limits. The package must be designed to confine the high level radioactive waste for the duration of the license." The federal regulations in 10 CFR 72 thus make it clear that fuel retrievability is a requirement, and, therefore, must be addressed in extended storage and transportation. Argonne gave a presentation on "Review of High-Burnup Fuel and Cladding Property Studies" (Billone and Liu) that included an update of the revised Argonne test plan for ring compression testing. Argonne is a member of the EPRI/ESCP Subcommittee on Cladding Issues and participated in the Subcommittee discussion during the breakout sessions.

5. REFERENCES

Aomi, M., Baba, T., Miyashito, T., Kaminura, K., Yasuda, T., and Shinohara, Y. 2008. "Evaluation of Hydride Reorientation Behavior and Mechanical Properties for High-Burnup Fuel-Cladding Tubes in Interim Dry Storage." J. ASTM International, Vol. 5, No. 9, Paper ID JA1101262; available online at www.astm.org.

Beyer, C.E. and Montgomery, R. 2011 "Post-Irradiation Cladding Characteristics." Presentation given at the Cladding Workshop, DOE-NE Used Fuel Disposition Campaign, Las Vegas, NV, November 15-17, 2011.

Billone, M.C. 2011 *Assessment of Current Test Methods for Post-LOCA Behavior*. NUREG/CR-XXXX, ANL-11/52. Currently in draft form and under review by NRC-NRR and NRC-NRO with publication date set for January 2012.

Billone, M., Yan, Y., Burtseva, T., and Daum, R. 2008. *Cladding Embrittlement during Postulated Loss-of-Coolant Accidents*. NUREG/CR-6967. [ML082130389 at http://www.nrc.gov/reading-rm/adams.html]

Burtseva, T.A., Yan, Y., and Billone, M.C. 2010. "Radial-Hydride-Induced Embrittlement of High-Burnup ZIRLO Cladding Exposed to Simulated Drying Conditions." ANL letter report to NRC, June 20, 2010. [ML101620301 at http://www.nrc.gov/reading-rm/adams/web-based.html]

Einziger, R.E. 2011 "Progress and Results of NRC's Cladding Programs." Presentation at the Technical Exchange Meeting sponsored by the Division of Spent Fuel Storage and Transportation, Office of Nuclear Material Safety and Safeguards, Nuclear Regulatory Commission, Washington, D.C., November 1, 2011.

Geelhood, K.J., Beyer, C.E., and Luscher, W.G. 2008. *PNNL Stress/Strain Correlation for Zircaloy*. PNNL-17700, July 2008.

Hanson, B., Alsaed, H., Stockman, C., Enos, D., Meyer, R., and Sorenson, K. 2011. "Gap Analysis to Support Extended Storage of Used Nuclear Fuel." DOE-NE Used Fuel Disposition Campaign report FCD-USED-2011-000136, June 30, 2011 draft.

Kessler, J., 2011 "Review of Gap Analyses and Priorities (as of August 2011)." Presentation at the Extended Storage Collaboration Program Meeting, Charlotte, NC, December 6-8, 2011.

Nakatsuka, M., Une, K., Tokunaga, K., and Ohta, T. 2004. "Mechanical Properties of High Burnup BWR Fuel Cladding Tubes under Simulated RIA Conditions." Proc. LWR Fuel Performance Meeting, Orlando, FL, Sept. 19-22, Paper 1017, pp. 526-535.

Nuclear Regulatory Commission 2003 Interim Staff Guidance (ISG)-11, Revision 3, "Cladding Considerations for the Transportation and Storage of Spent Fuel," November 2003.

Tsai, H., and Billone, M.C. 2003. "Characterization of High-Burnup PWR and BWR Rods, and PWR Rods after Extended Dry-Cask Storage." Proc. 2002 Nuclear Safety Research Conf., U.S. NRC, NUREG/CP-0180, pp. 157-168.

Yan, Y., Burtseva, T.A., and Billone, M.C. 2009 "Post-quench Ductility Results for North Anna High-burnup 17×17 ZIRLO Cladding with Intermediate Hydrogen Content." ANL letter report to NRC, April 17, 2009. [ML091200702 at http://www.nrc.gov/reading-rm/adams.html]

APPENDIX

Provisional Test Plan for High-Burnup Fuel Cladding and Modeling

December 31, 2011

Provisional Test Plan for High-Burnup Fuel Cladding and Modeling

for DOE/NE Used Fuel Disposition Campaign Research and Development

Argonne National Laboratory
December 31, 2011

PURPOSE

The purpose of this test plan is to generate data and models to support the development of the technical basis for extended long-term storage and transportation of used nuclear fuel.

In particular, the goal of this program is to determine drying/transfer and early stage storage conditions that will allow commercial-reactor, high-burnup used fuel cladding to maintain ductility during extended storage and transportation. For each set of conditions, ductility vs. ring compression test (RCT) temperature data and curves will be generated to allow determination of the ductile-to-brittle transition temperatures (DBTTs) of the cladding alloys. The primary goal would be achieved by determining drying/transfer and storage conditions for which the DBTT is <20°C following extended long-term storage. These drying/transfer-storage conditions or limits corresponding to DBTT <20°C may be too low for some cladding alloys to be practical. However, the resulting data will be useful to DOE and other stakeholders (e.g., utilities, cask vendors, etc.) in evaluating trade-offs among drying processing conditions, cask thermal loading and peak cladding temperature, and transport temperature for which cladding retains ductility.

1.0 BACKGROUND

Conditions that may lead to radial-hydride formation and cladding embrittlement are described in Section 5.2.3.5 of the draft report *Gap Analysis to Support Extended Storage of Used Fuel* (Hanson et al. 2011). The importance of conducting R&D in this area is ranked as high (see Table S-1 of Hanson et al. [2011]). The high ranking for closing this data gap is because maintaining ductility is important to preventing shattering of the cladding and fuel dispersal during handling and cask-drop accidents. For side-drop accidents, it is important to maintain ductility in response to both axial stresses due to bending and hoop stresses due to crush- or pinch-type loads at grid spacers and other locations along the fuel rod. Irradiation to high burnup results in reduced cladding ductility in the axial and hoop directions. Hydrogen redistribution during drying/transfer operations and early stages of storage, and hydrogen precipitation during very slow, long-term cooling can result in enhanced embrittlement in the hoop direction at storage temperatures below 200°C due to radial-hydride precipitation. The extent of radial-hydride precipitation and embrittlement depends on peak drying/transfer-storage temperatures and corresponding fuel-rod-internal gas pressures. Under Nuclear Regulatory Commission Interim Staff Guidance (ISG) 11, Rev. 3 (2003), the peak temperature for drying/transfer and storage is limited to 400°C. At this peak temperature, cladding hoop stresses would be ≤160 MPa for PWR cladding and ≤120 MPa for BWR cladding. These peak values are based on conservative fuel-vendor calculations of gas release. Most high-burnup fuel rods have internal pressures and corresponding hoop stresses well below the design-limit values. Thus, relevant cladding hoop stresses for this testing program are 80 to 160 MPa for PWR cladding, and 60 to 120 MPa for BWR cladding.

On April 28, 2011, Argonne issued a three-year test plan ("Provisional Test Plan for High-Burnup Cladding and Modeling") to address the data gap. The term "Provisional" means that tests will be

conducted sequentially with conditions for the subsequent test determined from the results of the previous test. The current test plan includes revisions based on new assessments of cladding hoop stresses for PWR and BWR cladding and on data generated by Argonne on high-burnup M5® for DOE since July 2011. This revised test plan is divided into four components: (a) Baseline Studies, (b) Testing at ISG-11 (Rev. 3) Limits, (c) Testing at Less than ISG-11 (Rev. 3 limits) and (d) Modeling.

2.0 BASELINE STUDIES

These tests remain basically the same as the ones proposed in the April 28 test plan, with the exception of the addition of high-burnup Zry-2 to the test matrices planned for high-burnup PWR alloys Zry-4, ZIRLO™, and M5®. The Zry-2 of interest is from fuel rods irradiated in one of the Limerick reactors to 65 GWd/MTU. Segments from these fuel rods may reside at GEH-VNC. One segment of each alloy will be used to run two axial tensile tests at room temperature (RT) and two strain rates (e.g., 0.1%/s and 100%/s). If a cladding alloy shows little strain-rate sensitivity, no further axial tensile tests will be required. For any alloy that shows significant strain-rate sensitivity, a third test will be conducted at >100%/s strain rate. The results of these studies will be used to determine mechanical properties (i.e., yield and ultimate strength and uniform and total elongation) of as-irradiated cladding prior to transfer from the pool, drying, and dry-cask storage. Axial tensile tests are summarized in Table 1.

Also included in the baseline studies of as-irradiated cladding are characterization and RT ring compression testing at three displacement rates (0.05 mm/s, 5 mm/s, and 50 mm/s). Establishment of the displacement- and strain-rate sensitivity is important for the following reasons: The displacement rate for pinch-type loading depends on the cask drop height, which varies from 0.3 m (normal transport) to 9 m (hypothetical accident during transport). If ductility decreases significantly with increase in strain rate, then such data are needed in extrapolating results from a 5 mm/s displacement rate to higher displacement rates. However, if ductility is a weak function of displacement rate, then it is more practical to use 0.05 mm/s for testing because displacement and load can be terminated following a significant load drop to determine permanent strain (from micrometer measurements) and crack depth into the wall (from metallography) corresponding to that load drop. As more than three rings will be available for each cladding segment, additional RCTs may be conducted at elevated temperatures and/or as repeat tests. For example, high-burnup M5® cladding with radial hydrides showed a significant increase in ductility at 90°C as compared to 60°C RCT test temperature. Thus, for this alloy, additional RCTs will be conducted at 60°C and 90°C and a 5 mm/s displacement rate to determine if as-irradiated cladding also exhibits such behavior. These baseline RCTs are summarized in Table 2.

Characterization (Table 3) will include metallographic imaging and hydrogen determination at both ends of the ≈80-mm-long cladding segments. Corrosion-layer thickness, metal wall thickness, hydride distribution across the cladding wall, and hydrogen content will be determined. For cladding alloys with a thick outer-surface oxide layer and hydride rim (i.e., Zry-4 and ZIRLO™), additional metallographic and hydrogen content measurements will be performed with the corrosion layer removed and with the corrosion/hydride-rim layers removed. A typical example under these baseline studies is shown in Figure 1 for a high-burnup Zry-4 segment with an estimated corrosion layer of ≈ 100 μm and a hydrogen content of ≈700 wppm. For M5® and Zry-2, which have neither a thick outer-surface corrosion layer nor a hydride rim, the sectioning diagrams will be modified accordingly. For Zry-2, the corrosion layer and the cladding inner-surface liner will be removed from one ring (e.g., C-D in Figure 1) to determine the average hydrogen content. That leaves six 8-mm-long samples for RCTs. For M5®, the outer-surface corrosion

layer will be removed from ring C-D. The remaining six 8-mm-long samples will be used for ring compression testing. For PWR cladding with a hydride rim, measurement of the average hydrogen content below the hydride rim is very important for gaining mechanistic understanding of the behavior of hydrogen during drying/transfer operations and storage. It is also important for pre-hydriding cladding and determining the degree to which pre-hydrided cladding is an adequate surrogate for high-burnup cladding.

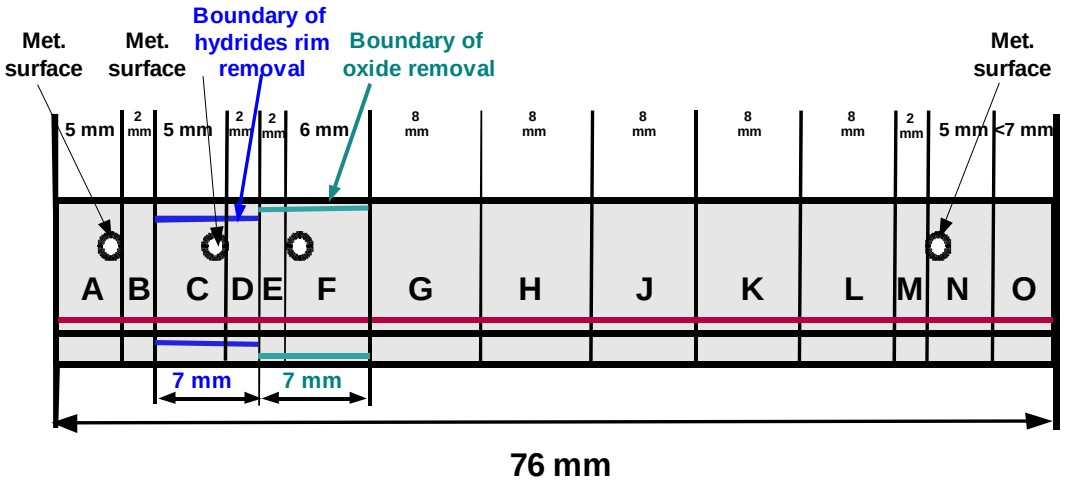

Figure 1. Sectioning diagram for baseline characterization and ring compression testing of a high-burnup Zry-4 cladding segment. Rings A, C, F, and N are metallographic samples with the white dots indicating the surfaces to be imaged. Rings B, D, E and M are for hydrogen content determination. Rings G-L are for ring compression testing.

Table 1. Matrix for axial tension tests to be conducted at room temperature (RT). Sample gauge length is 25 mm. HBR = H. B. Robinson, NA = North Anna, Lim = Limerick, and TBD = To Be Determined.

Material	H-content wppm	Temperature °C	Strain Rate %/s	Comment
HBR Zry-4 67 GWd/MTU	750±50	RT	0.1, 1.0 100 >100	Tests conducted for NRC --- TBD
NA ZIRLO™ 70 GWd/MTU	700±50	RT	0.1 100 >100	--- --- TBD
NA M5® 70 GWd/MTU	70±30	RT	0.1 100 >100	--- --- TBD
Lim Zry-2 65 GWd/MTU	300±50	RT	0.1 100 >100	--- --- TBD

Table 2. Ring compression test (RCT) matrix for as-irradiated cladding. Tests will be conducted to 1.7-mm total displacement with 8-mm-long rings. The first test will be conducted at room-temperature (RT) and the reference displacement rate of 5 mm/s.

Material	H-content wppm	RCT Temp °C	Displacement Rate, mm/s	Comment
HBR Zry-4	750±50	RT	5	---
67 GWd/MTU		RT	5	Repeat test
		RT	0.05	---
		RT	50	---
		TBD	TBD	---
NA ZIRLO™	700±50	RT	5	---
70 GWd/MTU		RT	5	Repeat test
		RT	0.05	---
		RT	50	---
		TBD	TBD	---
NA M5®	70±30	RT	5	---
70 GWd/MTU		60	5	Effects of test temperature
		90	5	Effects of test temperature
		RT	0.05	---
		RT	50	---
		TBD	TBD	---
Lim Zry-2	300±50	RT	5	---
65 GWd/MTU		RT	5	Repeat test
		RT	0.05	---
		RT	50	---
		TBD	TBD	---
		TBD	TBD	---

Table 3. Characterization of as-irradiated, high-burnup cladding. Metallography will be performed on post-RCT samples if there is visible evidence of cracking and/or if the load-displacement curve indicates a steep load drop >10%. Hydrogen content (H-content) measurements of post-RCT samples will be performed for segments that have significant axial variation in hydrogen content. OD = outer diameter, ID = inner diameter, Ox = oxide, and TBD = to be determined.

Material	HBR Zry-4	NA ZIRLO™	NA M5®	Lim Zry-2
H-content				
As-irradiated	2	2	2	2
OD Ox Removed	1	1	1	---
OD Ox/H-rim removed	1	1	---	---
OD-Ox/ID-Liner Removed	---	---	---	1
Post-RCT	TBD	TBD	TBD	TBD
Metallography				
As-irradiated	2	2	2	2
OD Ox Removed	1	1	1	---
OD Ox/H-rim removed	1	1	---	---
OD-Ox/ID-Liner Removed	---	---	---	1
Post-RCT	TBD	TBD	TBD	TBD

3.0 TESTING AT ISG-11 (REV. 3) LIMITS

Ring compression testing will be performed at drying/transfer-storage limits established by the NRC in ISG-11 (Rev. 3). These limits are: 400°C peak cladding temperature, <10 cooling cycles, and <65°C temperature drop per cooling cycle. Based on cask-vendor/utility experience with vacuum drying, only 3 to 5 cooling cycles would be needed. Also, a practical time interval between cooling cycles is about 24 hours. During this interval, the temperature drop will be >65°C. Thus, testing will be conducted for 1, 3 and 5 drying cycles with 100°C temperature drop per cycle.

The test matrices for testing at ISG-11 (Rev. 3) limits incorporated the experience from testing high-burnup Zry-4 and ZIRLO™ for NRC (Burtseva et al. 2010), and high-burnup M5® for DOE since July 2011 (Billone et al. 2011). High-burnup Zry-4 retained ductility at >60°C following 1-cycle simulated drying at a 400°C hoop stress of 140 MPa. At a 400°C hoop stress of 110 MPa, the DBTT for high-burnup Zry-4 was <20°C. To complete testing for this alloy, additional tests will be conducted on samples subjected to 3 and/or 5 temperature cycles from 400 to 300°C with a peak hoop stress of 110 MPa. For high-burnup ZIRLO™ subjected to simulated drying at 400°C hoop stresses of 140 MPa and 110 MPa, the DBTT values were >150°C and >100°C, respectively. It is clear from the work performed for NRC that the peak hoop stresses for high-burnup ZIRLO™ have to be reduced to <110 MPa. The next tests with ZIRLO™ will be conducted at a 400°C hoop stress of 80 MPa and 1, 3 and/or 5 temperature cycles with temperature drops from 400 to 300°C. The 80-MPa stress level is of particular significance to the guidance in ISG-11 Rev. 3, as the guidance implies that radial-hydride embrittlement should not occur at hoop stresses <90 MPa based primarily on data for pre-hydrided Zry-4. This stress threshold may not be valid for high-burnup cladding alloys, especially ZIRLO™, M5® and Zry-2. For high-burnup M5®, the 400°C hoop stress will also be reduced to 80 MPa. If there is a mixture of radial and circumferential hydrides under this simulated drying condition, then temperature cycling may be introduced for the next test. For high-burnup Zry-2, testing will be initiated at a 400°C hoop stress of 120 MPa. This stress will be reduced to 90 MPa and 60 MPa, if needed, to achieve a DBTT <20°C, or to minimize the DBTT. The results of these tests will be used to determine the 400°C hoop-stress level at which temperature cycling will be introduced.

The results of testing at the NRC ISG-11 (Rev. 3) limits will be a set of DBTT curves (offset strain vs. test temperature) for each set of simulated drying conditions of the high-burnup cladding alloys.

Table 4 summarizes the planned RCTs tests for high-burnup fuel cladding. Prior to conducting temperature-cycling tests with high-burnup Zry-4 and ZIRLO™, 1-cycle, 3-cycle, and 5-cycle tests will be conducted using non-irradiated, pre-hydrided cladding to determine the effects of number of cycles and if there is any significant difference in radial-hydride precipitation and hydrogen content below the cladding rim for 3 vs. 5 cycles. The results will be used to guide the number of cycles to be used in tests with high-burnup cladding listed in Table 4. It needs to be demonstrated that these non-irradiated cladding alloys can be pre-hydrided with <200 wppm hydrogen between the inside of the hydride rim and the cladding inner surface. The target hydrogen content is 400-600 wppm including the outer-surface hydride rim. However, samples with >600 wppm average hydrogen content would be acceptable as long as the cladding below the rim had <200 wppm hydrogen. Table 5 summarizes the non-irradiated, pre-hydrided tests for Zry-4 and ZIRLO™.

Table 4. Test matrix for simulated drying/transfer-storage conditions and ring compression tests (RCTs) for high-burnup cladding alloys. Four RCTs will be conducted for each cladding rodlet subjected to a simulated drying/transfer-storage condition. The first RCT will be conducted at 20°C. Subsequent RCT temperatures depend on the results of the first test.

Material	Peak Drying T, °C	Peak Drying σ_θ, MPa	# of Drying Cycles	RCT T, °C	Comment
HBR Zry-4	400	140	1	20-150	DBTT >60°C (NRC Work)
		110	1	20-150	DBTT <20°C (NRC Work)
		110	3 or 5	≥20	Is DBTT <20°C
NA ZIRLO™	400	140	1	20-200	DBTT >150°C (NRC Work)
		110	1	20-150	DBTT >100°C (NRC Work)
		80	1	≥20	Is DBTT < 20°C?
		80	3 or 5	≥20	---
NA M5®	400	140	1	20-150	DBTT = 80°C (DOE Work)
		110	1	20-90	DBTT = 70°C (DOE Work)
		80	1	≥20	Is DBTT < 20°C?
		80	3 or 5	≥20	---
Lim Zry-2	400	120	1	≥20	Is DBTT <20°C?
		90	1	≥20	If First-test DBTT >20°C
		60	1	≥20	If Second-test DBTT >20°C
		TBD	3 or 5	≥20	Likely at 90 or 60 MPa

Table 5. Test matrix for non-irradiated, pre-hydrided Zry-4 and ZIRLO™ with <200 wppm hydrogen between hydride rim and cladding inner surface. Multiple drying cycles involve temperature decreases from 400°C to 300°C. RCT = ring compression test.

Material	Peak Drying T, °C	Peak Drying σ_θ, MPa	# of Drying Cycles	RCT T, °C	Comment
15×15 Zry-4	400	110	1	≥20°C	Expect DBTT <20°C 4 RCTs
	400	110	3	≥20°C	4 RCTs
	400	110	5	≥20°C	4 RCTs
	400	TBD	3 or 5	≥20°C	Conduct only if DBTT >20°C for previous 2 tests
17×17 ZIRLO™	400	80	1	≥20°C	Expect DBTT <20°C 4 RCTs
	400	80	3	≥20°C	4 RCTs
	400	80	5	≥20°C	4 RCTs

4.0 TESTING AT LESS THAN ISG-11 (REV. 3) LIMITS

In testing at less than ISG-11 (Rev. 3) limits, the peak cladding temperature limit of 400°C in ISG-11 (Rev. 3) will be reduced to determine if higher stresses can be achieved while maintaining DBTT <20°C, or at least minimizing DBTT to the same levels determined in testing at the ISG-11 (Rev. 3) limits. Tests will first be conducted at a peak drying temperature of 350°C to determine the benefit with regard to peak hoop stress at that temperature. The stress levels used in the initial tests will depend on the results obtained in the testing at the ISG-11(Rev. 3) limits in Table 4. If a significant increase (e.g., 30 MPa) in allowable stress results from this decrease in peak drying temperature, a second set of tests may be conducted at 325°C. Drying temperatures <300°C can be achieved with forced helium-flow dehydration. However, peak temperatures lower than 325°C may be too restrictive with regard to cask loading and heating rate. Both non-irradiated, pre-hydrided and high-burnup cladding will be used in the testing at less than the ISG-11 (Rev.3) limits. Test matrices will be similar to the ones shown in Tables 4 and 5, except that the peak drying temperature will be reduced and the peak drying stress will be increased.

Although the goal of the ring compression testing of high-burnup fuel cladding is to determine drying/transfer-storage conditions for which DBTT <20°C, this goal may not be achievable for all cladding alloys at peak temperatures and stresses that are acceptable and/or practical. Regardless of whether this goal can be achieved, however, the DBTT data generated will allow informed tradeoffs between drying/transfer-storage conditions and post-storage retrieval and transportation temperatures.

5.0 MODELING

Cladding materials modeling and canister/cask modeling will be conducted in parallel with the test program. Materials modeling will include the following: (a) precipitation temperature of hydrides during cooling under stress; (b) stress-strain behavior under hoop bending loading of the composite cladding material containing brittle hydrides in a low-ductility matrix; (c) correlation between measured ductility (δ_p/D_o) of the cladding and the local plastic deformation in cladding prior to and after developing wall cracks; (d) correlation between change of cladding stiffness slope and crack depth into the cladding for rings that crack during the linear cladding deformation mode; (e) correlation between magnitude of steep load drop during elastic-plastic deformation and crack depth into the cladding wall (i.e., crack depth as a fraction of cladding wall thickness vs. percentage of load drop); and (f) condition of cladding with a 50% wall crack in response to pressure-induced hoop stress and axial bend stresses. The background for item (b) is documented by Billone (2011). Billone showed that within the elastic deformation regime, the elastic strain calculated by δ_p/D_o is three times the maximum elastic strain (ε_e) in the cladding material. While δ_p/D_o (with <2% strain indicating brittle behavior) is a useful metric using the RCT as a ductility screening test, it does not represent the local ductility in the cladding.

With regard to canister/cask modeling, this activity will be coordinated with colleagues from other DOE laboratories developing canister/cask thermal and mechanical models. Radial-hydride formation is highly dependent on fuel rod internal pressure, peak cladding temperature, and axial distribution of cladding temperature during drying/transfer and early stages of storage. If such modeling calculations are not provided, Argonne will use existing codes, such as ANSYS and FLUENT, to perform thermal calculations to estimate the peak cladding temperatures of used fuel assemblies within a canister or cask during drying/transfer and early stages of dry-cask storage. Argonne will also use existing codes, such as

ABAQUS and LS-DYNA, to perform structural calculations to evaluate the mechanical response of used fuel assemblies during drops of a canister/cask under normal conditions of transport and hypothetical accidents, using mechanical properties data determined from the cladding testing program and material modeling.

REFERENCES

Billone, M.C. 2011 *Assessment of Current Test Methods for Post-LOCA Behavior*. NUREG/CR-XXXX, ANL-11/52. Currently in draft form and under review by NRC-NRR and NRC-NRO with publication date set for January 2012.

Billone, M.C., Burtseva, T.A., Dobrzynski, J.P., McGann, D.P., Byrne, K., Han, Z. and Liu, Y.Y. 2011 *Phase I Ring Compression Testing of High-Burnup Cladding*. DOE-NE Used Fuel Disposition Campaign report FCRD-USED-2012-000039, December 31, 2011.

Burtseva, T.A., Yan, Y., and Billone, M.C. 2010. "Radial-Hydride-Induced Embrittlement of High-Burnup ZIRLO Cladding Exposed to Simulated Drying Conditions." ANL letter report to NRC, June 20, 2010. Publicly available as ML101620301 at http://www.nrc.gov/reading-rm/adams/web-based.html.

Hanson, B., Alsaed, H., Stockman, C., Enos, D., Meyer, R., and Sorenson, K. 2011. *Gap Analysis to Support Extended Storage of Used Nuclear Fuel* DOE-NE Used Fuel Disposition Campaign report FCD-USED-2011-000136, June 30, 2011 draft.

Nuclear Regulatory Commission 2003. Interim Staff Guidance (ISG)-11, Revision 3, "Cladding Considerations for the Transportation and Storage of Spent Fuel," November 2003.

Appendix E
FCT Document Cover Sheet

Name/Title of Deliverable/Milestone	UFDC R&D ES&T L2 Report
Work Package Title and Number	ST Engineering Materials Experimental - ANL
Work Package WBS Number	FT12-AN080508
Responsible Work Package Manager	Yung Liu (Name/Signature)

Date Submitted 1/10/2012

Quality Rigor Level for Deliverable/Milestone	☐ QRL-3	☒ QRL-2	☐ QRL-1 ☐ Nuclear Data	☐ N/A*

This deliverable was prepared in accordance with Argonne National Laboratory
(Participant/National Laboratory Name)

QA program which meets the requirements of
☒ DOE Order 414.1 ☐ NQA-1-2000

This Deliverable was subjected to:

☒ Technical Review ☐ Peer Review

Technical Review (TR)
Review Documentation Provided
☐ Signed TR Report or,
☐ Signed TR Concurrence Sheet or,
☒ Signature of TR Reviewer(s) below

Peer Review (PR)
Review Documentation Provided
☐ Signed PR Report or,
☐ Signed PR Concurrence Sheet or,
☐ Signature of PR Reviewer(s) below

Name and Signature of Reviewers

Dr. Hanchung Tsai (Argonne National Laboratory)

Digitally signed by Hanchung Tsai
DN: cn=Hanchung Tsai, o=ANL, ou=DIS, email=htsai@anl.gov, c=US
Date: 2012.01.10 09:20:37 -06'00'

*Note: In some cases there may be a milestone where an item is being fabricated, maintenance is being performed on a facility, or a document is being issued through a formal document control process where it specifically calls out a formal review of the document. In these cases, documentation (e.g., inspection report, maintenance request, work planning package documentation or the documented review of the issued document through the document control process) of the completion of the activity along with the Document Cover Sheet is sufficient to demonstrate achieving the milestone. QRL for such milestones may be also be marked N/A in the work package provided the work package clearly specifies the requirement to use the Document Cover Sheet and provide supporting documentation.